International Journal of Precision Engineering and Manufacturing-Green Technology (2021) 8:1061–1081
https://doi.org/10.1007/s40684-020-00250-2

Online ISSN 2198-0810
Print ISSN 2288-6206

REVIEWPAPER

Harvesting Electricity from CO_2 Emission: Opportunities, Challenges and Future Prospects

Peter Adeniyi Alaba[1] · Shaukat Ali Mazari[2] · Hamisu Umar Farouk[3] · Samuel Eshorame Sanni[4] · Oluranti Agboola[4] · Ching Shya Lee[1,5,6] · Faisal Abnisa[7] · Mohamed Kheireddine Aroua[8,9] · Wan Mohd Ashri Wan Daud[1]

Received: 25 November 2019 / Revised: 6 July 2020 / Accepted: 8 July 2020 / Published online: 29 July 2020

Abstract

The ever-increasing CO_2 emission has necessitated the search for suitable technologies for CO_2 utilization at a low cost. Recently, a novel concept called reactive gas electrosorption (RGE) for energy harvesting from CO_2 emission, which could boost the efficiency of a thermal power plant by 5% was proposed by Hamelers and coworkers. The concept involves mixing of air stream with a low CO_2 concentration with a stream of high CO_2 concentration in an alkaline aqueous electrolyte. However, this concept is faced with the challenges of designs specific for CO_2-electrolyte, and inadequate performance of the electrode materials. Therefore, this study showcases electricity generation opportunities from CO_2 via RGE and discussed challenges and prospect. The study reveals that the drawback relating to the electrode could be solved using heteroatom doped traditional carbon materials and composite carbon-based materials, which has been successfully used in capacitive cells designed for desalination. This modification helps to improve the hydrophilicity, thereby improving electrode wettability, and suppressing faradaic reaction and co-ion repulsion effect. This improvement could enhance the charge efficiency, sorption capacity durability of electrodes and reduce the energy loss in RGE. Moreover, intensification of the membrane capacitive deionization (MCDI) process to obtain variances like enhanced MCDI and Faradaic MCDI. Hybrid capacitive deionization (HCDI) is also a promising approach for improvement of the capacitive cell design in RGE. This intensification can improve the electrosorption capacity and minimize the negative effect of faradaic reaction. The use of alternative amine like Piperazine, which is less susceptible to degradation to boosting CO_2 dissolution is also suggested.

Keywords CO_2 energy · CO_2 utilization · Electrosorption · Capacitive cell · Reactive gas electrosorption

✉ Peter Adeniyi Alaba
peteradeniyi@um.edu.my; adeniyipee@email.com

✉ Ching Shya Lee
leecs@um.edu.my

✉ Wan Mohd Ashri Wan Daud
ashri@um.edu.my

[1] Department of Chemical Engineering, Faculty of Engineering, University of Malaya, 50603 Kuala Lumpur, Malaysia

[2] Department of Chemical Engineering, Dawood University of Engineering and Technology, New M.A Jinnah Road, Karachi 74800, Pakistan

[3] Department of Pure and Industrial Chemistry, Faculty of Physical Sciences, College of Natural and Pharmaceutical Sciences, Bayero University Kano, P.M.B 3011, Kano State, Nigeria

[4] Department of Chemical Engineering, Covenant University, P.M.B 1023, Ota, Nigeria

[5] University of Malaya, 50603 Kuala Lumpur, Malaysia

[6] UMR5503 Laboratoire de Génie Chimique (LGC), Toulouse, France

[7] Department of Chemical Engineering and Materials Engineering, Faculty of Engineering, King Abdulaziz University, Rabigh 21911, Saudi Arabia

[8] Research Centre for Nano-Materials and Energy Technology (RCNMET), School of Science and Technology, Sunway University, 47500 Bandar Sunway, Malaysia

[9] Department of Engineering, Lancaster University, Lancaster LA1 4YW, UK

1 Introduction

The ever increasing industrial and agricultural activity, as well as population growth, has propelled a corresponding increase in the demand for renewable and sustainable clean energy [1]. The success of this quest could significantly alleviate CO_2 emission in industrial sectors like fertilizer, paper, steel, cement, iron or petrochemical, and power sectors like gas, oil or coal.

Kudos to Hamelers and co-workers [1–3] for their recently discovered technology that generates electricity from the mixing of air and CO_2 emissions using capacitive cell. This technology is called Reactive Gas Electrosorption (RGE). RGE technology utilizes capacitive electrode cell pairs, like those used in capacitive deionization (CDI) or supercapacitors during water desalination. The process involves mixing of aqueous solutions with various salinities [3, 4]. For instance, mixing seawater with freshwater from rivers could generate energy of about 3 kJ/L of the freshwater [5]. In the same vein, when air from the atmosphere with a low CO_2 concentration is mixed with a gas stream with a high concentration of CO_2 (like exhaust gas from power plants), mixing energy is released, and electricity is generated. The released mixing energy is due to the reduction in the Gibbs energy content of the mixture lower than that of the two CO_2 streams.

Previously, electricity has been generated by mixing aqueous solutions with different salinity [4, 6]. The study of Post et al. [5] revealed that about 3 kJ/L of freshwater work is obtainable by mixing freshwater from rivers with seawater. Conversion of mixing energy to electricity has been explored using several technologies, like ion-selective porous electrodes [7–9], double-layer expansion [10] ion-selective membranes [6] and semipermeable [3]. Recently, the use of capacitive electrode cell pairs-based technology, like those used in CDI for water desalination [11–13] or supercapacitors [14, 15] has been explored.

Hamelers et al. [3] investigated the possibility of harvesting electricity from CO_2 emission from industries that generate flue gas with 5–20% CO_2 by mixing with air, which contains about 0.039% in aqueous electrolytes in a CDI cell. Their report shows that electrical energy could be generated from mixing air and CO_2 emissions. Previously, CDI technology has been employed in Post-combustion CO_2 capture using monoethanolamine (MEA) to minimize the heat duty required to regenerate MEA in the stripper [16]. The CDI system receives the CO_2-rich solution directly from the absorber column to adsorbed ionic species at oppositely charged electrodes during the charging cycle, and an ion-free solution is returned to the absorber, while the absorbed concentrated ions solution from the CDI is sent to the stripper for low heat duty regeneration. Incorporation of CDI to post-combustion CO_2 capture can conserve about 10–45% of the total energy supplied to the stripper, as well as reduce the size of the stripper, thereby minimizing the initial cost of CO_2 capture system [16].

To further develop the new technology, [3, 17] performed a theoretical study and open-circuit voltage computation using a pair of charge–selective capacitive electrodes. This advance gives an insight into the system behavior using water or MEA as a solvent, towards optimizing the process efficiency. However, the capacitive technology is characterized by intermittent operations, which include electrosorption of ions from the electrolyte solution followed by solvent regeneration, making the system to be somewhat complicated and costly. Porada et al. [1] explored the possibility of continuous capacitive technology using novel cylindrical ion-exchange membranes as flow channels. Rather than using the usual fixed-film electrodes, flow electrodes were used to enable continuous operation, making the system more straightforward and more stable to implement.

Despite the various improvement on the capacitive technology, several issues need to be addressed since the technology is still in its infancy. The design of the direct gas capacitive cell, as well as material development for electrode, needs to be improved to reduce production cost and energy loss. RGE was first carried out using water as a solvent, but the solubility of CO_2 in water is too low, thereby producing low power density (mW/m^2) [1, 2]. To improve the power density, MEA has been used as an alternative in harvesting energy because the solubility of CO_2 in MEA is higher compared to distilled water. The use of MEA also helps to reduce energy loss to some extent. However, MEA is susceptible to oxidative degradation in the presence of dissolved oxygen, catalyzed by iron, and carbamate polymerization and thermal degradation which occur in the stripper at high temperature during the regeneration process [18]. Interaction of flue gas with MEA in RGE could lead to evolution of ammonia, which consequently degrades the solvent, making it reusable. The imine radical in the system could interact with oxygen to form the peroxide radical and could produce hydrogen peroxide and imine, which hydrolysis to form hydroxyacetaldehyde and ammonia. Imine could also be transformed to ammonia and formaldehyde via oxidative fragmentation [18]. Therefore, it is necessary to formulate solvent/electrolyte that is less susceptible to degradation. Furthermore, the electrosorption capacity obtained using porous carbon is not enough to meet the demand of the practical application. Therefore, it is urgently necessary to rationally designed/modified electrodes with enhanced microstructure for RGE application.

This work gives an overview of the opportunities, challenges and prospect of the RGE technology. We discussed and recommended the use of alternative solvents with high

CO_2 solubility but less susceptible to degradation when compared with MEA. The use of oxidative degradation inhibitor is also discussed. Development of electrode materials with enhanced electrosorption capacity and can produce high power density with low ohmic resistance is also critiqued.

2 Capacitive Technology

Capacitive technology entails extraction of mixing energy from two solutions with different concentrations using capacitive electrode cells either in a process known as capacitive mixing (CAPMIX) or capacitive deionization (CDI). CAPMIX emanated from the effort of the European Union towards the deployment of porous capacitors for Blue Energy development [19]. By this technology, electricity is produced using salinity gradients systems via the mixing of sea and river water [10]. Capacitive cell system comprises a pair of porous carbon electrodes (PCEs) sandwiched with a spacer channel, which enables the flow of electrolyte. The porous structure of PCEs enables accumulation of ion due to electrical double layers (EDLs) formation in the micropore, which is efficient storage for capacitive energy [20]. Therefore, capacitive deionization [12, 21] and EDL capacitors (supercapacitors), which are used for energy storage are fabricated using porous carbon materials [22–24]. PCEs act as an anode–cathode pair when an external electric potential is developed between the electrodes to attract and accumulate anions and cations. CDI is a room temperature and low-pressure process that involves flowing of water through or between electrodes as potential is applied. When the applied potential is positive, electrosorption occurs via a chemical reaction with the electrode material or EDL adsorption [25]. When the potential is reversed or released, the absorbed ions are forcedly removed from the electrodes, thereby regenerating them for the successive cycles. Furthermore, CDI is a cost-effective technology that could be easily renewed and operates at a low energy consumption since it uses electrostatic force [26, 27]. It does not generate secondary pollution, as compared with current desalination techniques, and the energy recovery potential from the charge stored in the electrodes during the sorption process [28, 29].

The efficiency of CDI process based on carbon materials can be improved by incorporating ion exchange membranes in a configuration called membrane CDI (MCDI). However, like supercapacitors, carbon-based materials are limited in their capacity to adsorb salt by the surface area available for electrosorption [28–30]. This drawback can be overcome by using electrode materials capable of faradaic reactions with the ions in the electrolyte. Faradaic reactions are not limited by surface area since they can occur all through the bulk of the structure [31].

The electrons flowing through the electric conductors and the external circuit from one electrode to the other were used to balance the ionic charge. When solutions of different ionic composition are charged into a capacitive cell alternatingly, electrical energy can be produced from the spontaneous ionic current induced by membrane potential generated from a set of anion- and cation-exchange membranes are placed between the PCEs and the spacer channel [17].

3 Reactive Gas Electrosorption (RGE)

Reactive Gas Electrosorption (RGE) was a recently introduced technology Hamelers and co-workers [1–3] for CO_2 capture and utilization to generate electricity by mixing of CO_2 emissions and air using capacitive technology. RGE technology was inspired by an existing technology that uses capacitive cells to extract energy from mixing of seawater with river water; a process referred to as CAPMIX [8, 21]. This technology involves reactive ionic transportation of chemical species in porous carbon electrodes (PCEs) via ion-exchange membranes (IEMs), leveraging on gradients of electric and/or chemical potentials.

Like MCDI, the components of RGE includes PCEs, IEMs, a solvent/electrolyte (Fig. 1) [2]. The PCEs stores

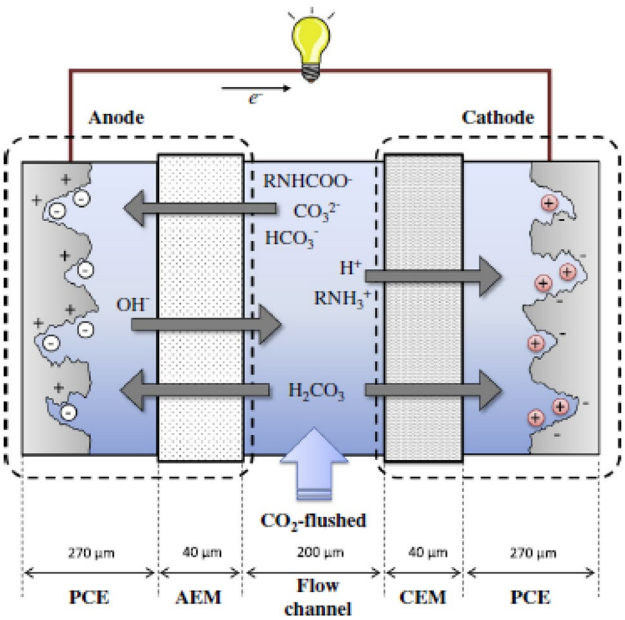

Fig. 1 Schematic picture of the capacitive cell (operating in the charging step) [17]

ions and engender a flow of electrons, while the IEM [anion-exchange membrane (AEM), and cation exchange membrane (CEM)] generates a potential in contact with different concentration of ions. The solvent is required for dissolution of CO_2 into ions. The concentration of the produced ions largely depends on the pressure of the fed CO_2. In the electrolyte, CO_2 interacts with water to evolve carbonic acid, which latter dissociates to form bicarbonate ions (HCO_3^-) and protons (H^+) as in Eq. 1. At high pH (in the presence of amine), the HCO_3^- dissociates to carbonate ions (CO_3^{2-}) as in Eq. 2. If pure water is used as the electrolyte, only Eqs. 1 and 3 occur, while Eqs. 1–5 occur when amine is used. $RNHCOO^-$, CO_3^{2-}, OH^- and HCO_3^- migrate to the anode, while H^+, and RNH_3^+ migrate to the cathode. Electrical energy is generated due to the difference in the ion concentration between the CO_2-flushed solution and the air-flushed solution.

$$H_2CO_3^* \leftrightarrow H^+ + HCO_3^- \tag{1}$$

$$HCO_3^- \leftrightarrow H^+ + CO_3^{2-} \tag{2}$$

$$H_2O \leftrightarrow H^+ + OH^- \tag{3}$$

$$RNH_3^+ \leftrightarrow RNH_2 + H^+ \tag{4}$$

$$RNHCOO^- + H_2O \leftrightarrow RNH_2 + HCO_3^- \tag{5}$$

RGE technology is carried out in a capacitive cell using two different techniques [32]. RGE can be operated by capacitive mixing to produce electrical current based on the mixing CO_2 emission from power plant-based exhaust gas (10–20% CO_2) with an air stream (0.04% CO_2) and dissolving them in an electrolyte [32, 33]. RGE can also be operated using CDI cell technology by using an external energy supply to enable absorption and desorption of ions to and from the PCEs. Since the concentrations of ions in the electrolyte affect the dissolution of CO_2, the charging and discharging of the capacitive cell can either concentrate or capture the CO_2 gas stream [33].

The capacitive cell is operated intermittently, charging and discharging. At the charging step, the concentrated CO_2 solution is charged into the cell, and the ions flow into the micropores of the PCEs, where EDLs are formed [34]. Since the technology uses IEMs, only the cations could flow to the cathode (covered with CEM), while the anions mainly flow to the anode (covered with AEM) (Fig. 1). The electrons transfer through the external electrical circuit compensate the produced ionic current that flows to the cathode from the anode, also from anode to cathode, thereby setting up an electrical current [2]. At the discharging step, as dilute CO_2 solution is charged into the cell, the ions are released from the electrodes and flow through the IEMs back to the flow channel. Therefore, electrons stored in the cathode are released to generate electrical current once again, but in the opposite direction.

Despite the use of IEMs, non-hydrated CO_2 and undissociated H_2CO_3 find their way via the membranes by concentration gradients because they are not affected by the co-ion expulsion suppression of the IEMs [17]. Electrically, the capacitive cell functions as a capacitor and the system can be described using an RC equivalent circuit, as shown in Fig. 2 [17]. The IEMs are modelled considering the internal resistance and power supply a (or voltage source). The internal resistance depends on the IEM conductivity, and the power supplied is driven by a concentration gradient. The PCEs are also modelled considering a series arrangement of internal resistance and capacitor.

Using RGE technology, energy harvested from CO_2 emissions could potentially boost the efficiency of a thermal power plant by 5% [32]. This technology helps to generate more electricity from power plants without the usage of more fuel and further exhaust gas emission. However, RGE technology is in its infancy. Since the capacitive cell was previously designed for wastewater treatment, it is essential to provide scientific insight into the RGE process and conceive more suitable and facile designs for CO_2-electrolyte. Rational design of capacitive cell for RGE process could be achieved by reviewing the challenges and proposing possible solutions. Section 4 presents the challenges that lead to energy losses in the cell, and Sect. 5 suggests the potential panacea like the use more stable electrolyte and degradation inhibitors, synthesis of more suitable materials for fabrication of PCEs, and optimization of the cell configuration/architecture.

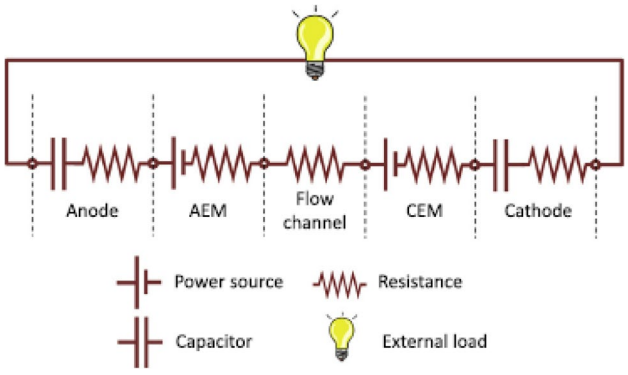

Fig. 2 Equivalent electrical circuit of the membrane-enhanced capacitive cell [17]

4 Challenges of Reactive Gas Electrosorption (RGE)

4.1 MEA Degradation

Initially, RGE technology was introduced with water as an electrolyte, in which CO_2 solubility is very low; hence, this compels the system to produce a low-density current. From the experiences of post-combustion CO_2 capture, we learn that CO_2 is highly soluble in MEA solutions. Unlike water, MEA is costly and requires regeneration. The current generation principle for the capacitive cell is based on the mixing process between an exhaust gas (from the selected plant) and an airstream dissolved into an electrolyte. The system either through flue gas or the air stream inherently introduces oxygen into it. Apart from oxygen, trace metals, NO_x, SO_x, fly ash, and other combustion particles come along with flue gas [35, 36]. The presence of oxygen, fly ash, and other fine particulate matters make the electrolyte vulnerable to irreversible reactions leading to its concentration loss [37]. The degradation products include nitric acid, formic acid, and oxalic acid [38], which could lower the pH of the solvent during RGE. Since the enhanced performance of MEA in RGE as compared with water is due to the high pH of MEA, the formation of degradation product could lower the performance of RGE.

Although with the aid of desulfurization devices and fabric or electrostatic filters, over 99.9% of fly ash could be removed from flue gas effluent of coal-fired power plant, the residual fly ash tends to accumulate during the CO_2 capture process [39–41]. The fly ash comprises inorganic oxides and transition metal elements like vanadium, chromium, iron, nickel and copper, which could catalyze amine degradation [38, 42, 43]. For instance, as low as 10 ppm of dissolved copper is enough to cause serious oxidative degradation of amine [39]. Likewise, as low as 0.0001 mM dissolved iron concentration in the flue gas can enhance oxidative degradation [18].

Typically, oxidative degradation is provoked by the presence of free radicals, which could be generated in large numbers in the presence of fly ash to accelerate the degradation rate. Either catalyzed or non-catalyzed oxidation degradation mechanism of MEA is similar (major products) but are in different ratios [39]. Therefore, MEA degradation induces extra cost and impacts the environmental balance of the RGE process and its efficiency.

4.2 Poor Performance of PCE

PCE is the heart of CDI and is generally fabricated using activated carbon nanofibers (ACF) [44, 45], activated carbon (AC) [46, 47], carbon aerogel (CA) [48], graphene [49, 50] and carbon nanotubes (CNTs) [51, 52]. Conventional carbon materials exhibit a range of limitations, like low electrical conductivity and low capacitance. Furthermore, materials like graphene with two-dimensional planar structure comprise conjugated carbon atoms, making it to theoretically exhibit ultrahigh specific surface area (SSA) (about 2600 $m^2\ g^{-1}$) with remarkable electrical conductivity (about 7200 m s^{-1} at room temperature) and EDL capacitance (21 μF cm^{-1}) [53, 54]. However, graphene exhibits poor performance in CDI due to its π–π interactions and Van der Waals, which induce restacking of graphene sheets [55, 56]. One of the strategies towards preventing graphene sheets from aggregating during reduction is by fabricating 3D graphene structure. Several authors have synthesized macroporous 3D graphene materials with slackly stacked graphene sheets, but the SSA is not high enough [29, 57]. Furthermore, the preparation strategies of 3D graphene materials are time-consuming, relatively complicated, and practically not cost-effective [29]. Therefore, it is essential to try to seek a simple and cost-effective strategy to synthesize novel graphene structure with enhanced electrosorption capacity for practical applications of RGE.

Generally, the limitation of conventional PCE is because of faradic reactions occurring at the electrode surface and co-ion expulsion effect. When voltage is applied using conventional PCE, the oppositely charged counter ions migrated to the surface of the electrode to repel the co-ions. This repulsion provokes simultaneous adsorption/desorption cycle, thereby increasing energy consumption and decreasing charge efficiency [58–60]. The faradaic reaction occurs in a capacitive cell when anodic oxidation of electrode occurs over a long period, resulting in electrode deterioration, declined electrosorption performance and excessive energy consumption [61].

4.3 Energy Loss

The decline associated with energy efficiency could be ascribed to ohmic (resistive) and non-ohmic (parasitic) losses. The ohmic losses are due to bulk resistance (Rs), charge transfer resistance (Rct) and Warburg impedance (Z_W), resulting from the resistance of imperfect electrodes and the nature electrolytes. Non-ohmic losses are ascribed to leakage of currents and parasitic electrochemical charge transfer resulting from Faradaic reactions 61.

The anode oxidation may be direct or indirect. Direct oxidation occurs following Eqs. (6)–(9) [62–64], while indirect oxidation is induced by the anodic formation of oxidants like HCO_3^- and hydroxyl radicals. Techniques like cyclic voltammetry (CV) [65, 66], scanning electron microscopy (SEM) with energy dispersive X-ray (EDX) mapping [67], acid–base

titration, Fourier transform infrared spectroscopy (FTIR), and X-ray photoelectron spectroscopy (XPS) [68, 69] can be used to monitor the changes in the functional group of the capacitive electrodes. Using XPS technique, Bouhadana et al. [68] and Cohen et al. [69] reported that redox reaction is confirmed by alteration in the response of carbon (C 1 s) and oxygen (O 1 s) to the charging and discharging cycling of the carbon cathode and anode. The intensity of the C 1 s spectrum decreased whereas the O 1 s intensity increased in the carbon anode after numerous cycle, revealing that the anode developed more oxygen holding functional groups during the capacitive operation. However, the oxygen species were partially recognized [68].

$$C + H_2O \rightarrow C = O + 2H^+ + 2e^- \tag{6}$$

$$C + H_2O \rightarrow C - OH + H^+ + e^- \tag{7}$$

$$C + 2H_2O \rightarrow CO_2 + 4H^+ + 4e^- E^0 = 0.21V/SHE \tag{8}$$

Anodic oxidation penalizes the porosity of PCEs (which significantly contributes to electrosorption capacity) during the continued charging-discharging cycles in capacitive cells, thereby increasing the resistivity [61, 70–72]. Therefore, it is critically essential to alleviate this Faradaic parasitic side reaction towards minimizing energy loss in capacitive cells.

When low current is applied, parasitic loss dominates the energy loss since the electrode maintains higher voltages for a more extended period. However, at high current, resistive energy drop becomes the dominant loss since it increases almost linearly as the current increases for fixed charge transfer [61, 73]. The report of Qu et al. [74] reveals that the energy loss in constant current (CC) mode is less significant operation when compared with that of constant voltage (CV) mode. This trend could be ascribed to longer charging time and higher resistive dissipation at higher oxidizing potentials.

5 Prospects

5.1 Use of Alternative Supporting Electrolyte

Amines are proved ionization agents for CO_2, MEA of is one of the examples. In an electrolyte of an amine system with CO_2, chemical changes occur between a nonbonding electron pair at the amino nitrogen atom and an antibonding empty orbital in CO_2 for a donor–acceptor interface. The reaction proposed for CO_2 and an amine is as under [75]:

$$CO_2 + R_1R_2NH \leftrightarrow R_1R_2NCOOH \tag{9}$$

$$R_1R_2NCOOH + B \leftrightarrow R_1R_2NCOO^- + BH^+ \tag{10}$$

where R_1 and R_2 are substituents attached to the amino nitrogen; B is a base molecule that can be OH^-, water, or an amine.

In these reactions, carbamic acid is formed initially, then followed by the formation of protons. Later selective electrodes may attract the respective ions to them, where they get accumulated storing more energy to the system.

Deionization of CO_2 contributes to its solubility in aqueous systems of amines. Hence, the higher the solubility, the higher shall be the capacity of deionization or vice versa. Capacity and rate of deionization vary with the chemistry of amines. Yang et al. [76] screened amine solvents for solubility of CO_2 using a wetted wall column setup. Authors conducted experiments on different amines at 40–100 °C with different CO_2 loadings. The CO_2 loading was based on CO_2 partial pressure of 500–5000 Pa at 40 °C. Comparative results of a study for different amines are tabulated as under (Table 1).

Screening results indicate that there are many viable solvents available compared to MEA. Piperazine (PZ) and its derivatives carry a better cyclic capacity and dissolution rate than the benchmark MEA. However, hindered amines show a proper CO_2 loading, but they have a slow dissolution rate. The flow of hindered amines may be increased by adding a promoter like PZ. The hindered amines also have higher cyclic CO_2 capacity, their application with an activator like PZ may make them suitable for the application. The higher cycling capacity of amines lowers the operational costs, which includes regeneration and makeup.

5.2 Oxidation Inhibitor

Degradation of MEA in RGE could be suppressed by using radical/O_2 scavengers or chelating agents or a combination of both. Potential oxidation inhibitors include N-HydroxyEthylDiamine TriAcetic acid (HEDTA), N,N-Dimethylmonoethanolamine (DMMEA), TriEthanolAmine (TEA), gluconate, glycine, bicine, potassium-sodium tartarate (KNaC4H4O6.4H2O), Ethylenediaminetetraacetic acid (EDTA) (Table 2) [78, 79]. Other promising inhibitors include citric acid, diethylenetriamine penta(methylene phosphonic acid) (DTPMP) and Etidronic acid, 1-hydroxyethane 1,1-diphosphonic acid (HEDP).

The activity of oxidation inhibitor towards prevention amine degradation depends on the targeted oxidation catalyst. For instance, Blachly and Ravner [80] reported that EDTA could effectively inhibit Cu^{2+}–catalyzed amine oxidation but EDTA could not effectively prevent ferric and ferrous catalyzed oxidation. Whereas 1.5 wt% of N,N-Diethanolglycine (bicine) could effectively suppress degradation catalyzed by Ni^{2+}, Cr, Fe^{2+}, and Fe^{2+} but not Cu^{2+}. However, Chi and Rochelle [18] reported that the effect of EDTA on ferric and ferrous catalyzed oxidation greatly depends on

Table 1 Loading capacity and CO_2 absorption rate of different amines under lean and rich loading conditions

Amine	Molal concentration (m)	Lean loading (mol CO_2/mol alkalinity)	Rich loading (mol CO_2/mol alkalinity)	Cyclic CO_2 Capacity (mol/kg (water + amine))	liquid film mass transfer coefficient (kg') avg@40 °C (×10 [7] mol/s·Pa·$m^{2)}$	Refs.
Piperazine (PZ)	8	0.31	0.39	0.79	8.5	[76]
N-methyl/PZ	8	0.16	0.26	0.83	8.4	[76]
Methydiethanolamine (MDEA)/PZ	5/5	0.21	0.35	0.99	8.3	[76]
MDEA/PZ	7/2	0.13	0.28	0.80	6.9	[76]
8 m 2-methyl PZ	8	0.27	0.37	0.93	5.9	[76]
MEA	7	0.45	0.55	0.47	4.3	[76]
Diglycolamine (DGA®)	10	0.41	0.49	0.38	3.6	[76]
N-methyl-1,3-propanediamine (MAPA)	8	0.47	0.51	0.42	3.1	[76]
2-amino-2-methylpropane (AMP)	4.8	0.27	0.56	0.96	2.4	[76]
N-(2-hydroxyethyl) piperazine (HEP)	7.7	0.15	0.24	0.68	5.3	[77]
1-(2-aminoethyl) piperazine (AEP)	6	0.26	0.3	0.66	3.5	[77]
2-piperidine ethanol (2-PE)	8	0.37	0.68	1.23	3.5	[77]

the concentration of the EDTA used (Fig. 3a). At steady state, 4.5 mM EDTA could decrease the rate of oxidation of amine-containing 0.2 mM Fe^{3+} by 40%. They also revealed that 100 mM of bicine could reduce the MEA (7 m) oxidation rate by a factor of 2 (Fig. 3b).

Furthermore, excellent inhibition could be achieved by combining different inhibitors. For instance, oxidative degradation of MEA could be decreased by a synergistic combination of radical scavengers DTPA or Inhibitor A and a chelating agent HEDP [81].

5.3 Modification of Conventional Carbon Materials

Capacitive cell has been operated using several carbon electrode materials like graphene [87], mesoporous carbon (MC) [88, 89], carbon nanofibers (CNFs) [44, 90], carbon spheres (CSs) [91], activated carbon (AC) [92, 93], carbon nanotubes (CNTs) [94, 95] and carbon aerogels (CAs) [96, 97]. However, traditional carbon materials exhibit poor supercapacitor and deionization application due to low adsorption capacity and high energy loss, thereby hindering the commercialization of capacitive process [94]. Therefore, a new technique is essential towards fabricating a more potent carbonaceous material for capacitive operation.

Modification of conventional carbon materials to produce sustainable, cost-effective and highly effectual composite electrodes is a promising technique that could improve the supercapacitor and deionization application of the electrode, thereby enhancing the performance of the RGE system [98, 99]. Rational modification of carbon materials can significantly influence the charge efficiency, energy loss, sorption capacity and durability of electrodes in RGE [100].

5.3.1 Composite Materials

Porous carbon materials can be combined with other active materials since they have tunable microstructure to achieve improved properties, thereby enhancing the electrocatalytic performance of PCEs [101]. Composite materials are fabricated by hybridizing two different carbon materials, modifying or systematically combining metal oxides with porous carbons. For instance, Xu et al. [102] fabricated hybrid hierarchical porous carbon nanotubes (CNTs)/porous carbon polyhedra (PCP) (hCNTs/PCP) for capacitive operation. The prepared (hCNTs/PCP) exhibits CNTs-inserted-PCP porous structure with better electrical conductivity, higher specific surface area relative to PCP and CNT, thereby demonstrating higher sorption capacity (20.5 mg g^{-1}) and cyclic stability. The report of Gao et al. [101] using hybrid carbon nanotube and carbon polyhedron (HCN) also shows the potency of hybrid carbon materials in capacitive operation. The fabricated HCN exhibits a remarkable performance with the best capacitance of 343 F g^{-1} (at10 mV s^{-1}) and excellent cyclic stability because HCN has a shorter ion diffusion path.

Porous carbon can be modified with metal oxides with hydrophilic functionality like MnO_2, TiO_2, ZnO, ZrO_2 and SiO_2 to improve the wettability of the electrode [59, 103]. Min et al. [59] investigated the suitability of TiO_2 coated AC synthesized by a sol–gel technique in a capacitive cell. They reported that TiO_2 coating shifted the potential

Table 2 Some inhibitors tested for oxidative degradation of MEA

Inhibitor	Strength	Weakness	Refs.
MDEA	Could reduce MEA degradation by ~ 80% by preferential reacting with O_2. Could reduce NH_3 formation by 90% at a MDEA concentration ≥ 20 wt%	MDEA degradation increases the degradation products; cannot stop MEA degradation; MDEA is only active at temperature > 100 °C	[81, 82]
Inhibitor A	Effective at inhibiting MEA degradation provoked by both Cu^{2+} and Fe^{2+}, more efficient than chelating agents like HEDP	Less effective at higher temperatures (70 °C)	[81, 83, 84]
Inhibitor B	Could reduce MEA degradation by 75% at 55 °C in the presence of Fe^{2+}	Not as efficient as inhibitor A	[85]
Na_2SO_3	Cheap inhibitor, competes with MEA for the available O_2 to form sulfate, thereby reducing NH_3 formation in in the presence of Fe^{2+} and Cu^{2+}	Not as efficient as a degradation inhibitor in comparison to inhibitor A	[83]
DMTD (2,5-dimercapto-1,3,4-thiadiazole)	Very efficient oxygen scavenger, more efficient than chelating agents like HEDP	It decreases the thermal stability of MEA, making it unacceptable for industrial application	[81, 86]
Diethylenetriaminepentaacetic acid (DTPA)		It decreases the thermal stability of MEA, exhibits high affinity for metal ion to favor corrosion, making it unrecommendable for RGE process	[81, 86]
DTDP (3,3′-dithiodipropionic acid)		It decreases the thermal stability of MEA, making it unacceptable for industrial application	[84]
HEDP (1-hydroxyethylidene diphosphonic acid)		Poor inhibitor of oxidative degradation owing to low thermal stability	[84]

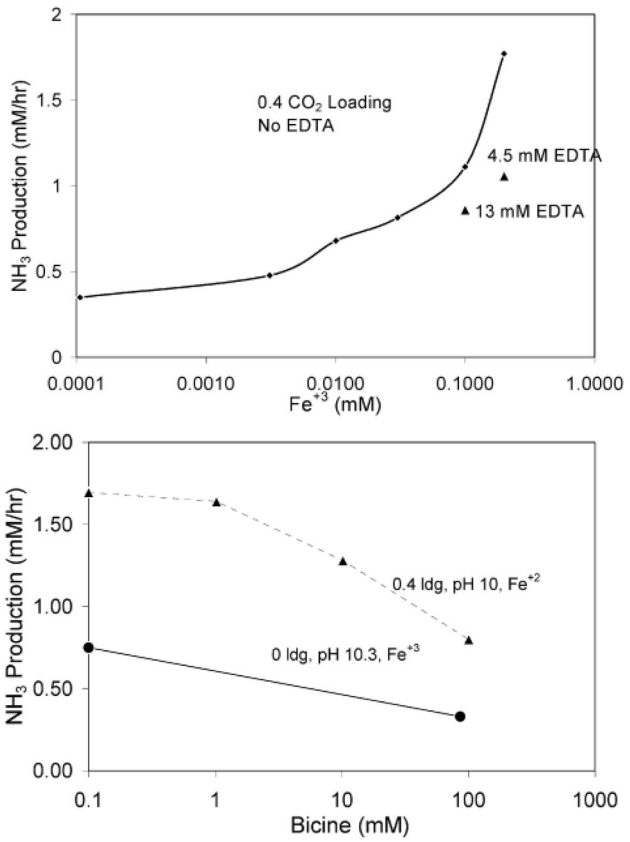

Fig. 3 Effect of **a** EDTA, **b** bicine in 7 m MEA with 0.4 mol CO_2/mol MEA, containing ferric or ferrous [18]

of zero charge (E_{PZC}) of the electrode to a more positive area. This shift increases the wettability and reduces the co-ion repulsion effect, thereby improving electrosorption capacity and charge efficiency. Yasin et al. [104] fabricated ZrO_2 nanofibers/AC composite as an electrode to conduct CDI test and reported a remarkable electrosorption capacity of ~ 16.35 mg g^{-1} at 1.2 V (compared to 5.42 mg g^{-1} for AC). When Yasin et al. [105] added TiO_2 and nitrogen doping to ZrO_2 nanofibers/AC (NACTZ) electrode, they reported electrosorption capacity of ~ 3.98 mg g^{-1}.

Also, essential metal oxides that can be used to functionalize the porous carbon materials are trivalent, and divalent metal cations called layered double hydroxides (LDHs). LDHs are anionic clay materials, which are cheap, durable and highly versatile in both morphology and composition [106, 107]. MgAl-LDH can be decomposed into corresponding mixed metal oxides by calcination to regenerate the original layered structure by anions absorption from the electrolyte into the interlayer. This regeneration process is called "memory effect" [108, 109]. Gao et al. [110] reported that graphene sheets and LDHs fabricated by the hydrothermal process have higher capacitive performance than the reference graphene. Ren et al. [111] prepared a simple technique for in situ hybridization of MgAl-Ox nanosheets on graphene (MgAl-Ox/G). The MgAl-Ox/G nanocomposite had high electrical conductivity, high surface area, and exceptional cyclic stability and high electrosorption capacity. These remarkable features are attributable to the memory effect and anodic oxidation suppression property of the material. Table 3 presents the comparative performance of conventional and composite PCE in capacitive cell configurations.

5.3.2 Modification by Heteroatom Doping

Heteroatom-doped carbon materials have become prominent electrode materials in electrochemical cells. In the past decades, N-doped hierarchical porous carbon (HPC) electrodes have been successfully used for electrochemical reactions, yielding promising material design [114, 115]. Doping of heteroatom on carbon material induces variation in spin densities and electronic charge densities in a carbon matrix, which disturbs the electroneutrality, thereby influencing the EDL [116, 117]. Prominent of all the heteroatom used is nitrogen. Nitrogen doping property enhances diffusivity of ion, fine wettability charge transferability and cycle stability [118–120]. However, it is essential to study the optimum amount of heteroatom in doping HPC to prevent the parasitic faradaic reaction. The parasitic faradaic reaction is caused by the presence of excess heteroatom and can affect the charge efficiency because some Coulombs of charges are not taking part in the EDL formation [93]. Lin et al. [121] rationally designed N-doped HPC electrodes and reported that the electrodes exhibit an excellent specific capacitance of ~ 855 F g^{-1}, delivering remarkable specific energy of 41.0 Wh kg^{-1} in aqueous electrolyte, which can be compared with those of lead-acid batteries.

Simultaneous doping of multiple heteroatoms can lead to the formation of more defect sites in the carbon matrix, thereby favouring the diffusion of ions and enriching carbon materials with electrons. In comparison with N-doped HPCs, multiple doped HPCs can generate a multiple functional group or multiatomic synergies, thereby improving the wettability and electrical conductivity of carbon materials [122–124]. Heteroatom doping can activate the stable carbon lattices, and multiple heteroatoms doping can deliver synergistic effects that could activate carbon matrix [125–127]. For instance, codoping sulfur and nitrogen on carbon spheres with a specific surface area of only ~400 m^2 g – 1 display excellent specific capacitance (295 F g^{-1} at 0.1 A g^{-1}) and rate capability (247 F g^{-1} at 10 A g^{-1}) [127].

Doping of multiple heteroatoms increases the active sites, and the synergistic effect of the co-doped heteroatoms on the electrode material can enhance the electrochemical kinetics and energy storage performance of a capacitive cell due to the development of the unique

Table 3 Comparative performance of conventional and composite PCE in capacitive cell configurations

Sample	Initial NaCl concentration (mg L^{-1})	Working potential (V)	Specific capacitance (F g^{-1})	Sorption capacity (mg/g)	Charge efficiency (%)	Refs.
PCP	1000	1.2	73.0	16.6	65	[102]
CNTs	1000	1.2	37.7	8.9	43	[102]
CNTs/PCP	1000	1.2	104.2	20.5	72	[102]
HCN	500	1.2	343	7.08		[101]
AC	500	1.2	192	6.9	61	[59]
AC-Ti	500	1.2	222	8.7	84	[59]
rGO	300	1.2	59	4.0	50	[112]
rGO/TiO_2	300	1.2	443	16.4	69	[112]
AC	100	1.2	44.9	5.4		[91]
AC/TiO_2	100	1.2	84.7	8.1		[91]
AC	104	1.2	207.46	5.42	16.37	[104]
ZrO_2 nanofibers/AC	104	1.2	869.86	16.35	53.26	[104]
TiO_2/ZrO_2 nanofibers	100 μS cm^{-1}	1.2	0.4	0.067		[105]
AC	100 μS cm^{-1}	1.2	207.46	1.4	25.44	[105]
ACTZ	100 μS cm^{-1}	1.2	251.32	2.96	53.08	[105]
NACTZ	100 μS cm^{-1}	1.2	691.78	3.98	71.19	[105]
Graphene aerogel	500	1.2	53.1	7.5	73	[113]
Graphene Aerogel/TiO_2	500	1.2	119.7	9.9	68	[113]

structural features [128]. However, the fabrication of multiple heteroatom doping of porous carbon could be complicated because tedious steps are involved and the need to control byproduct wastes. Therefore, it is vital to ensure facile, environmentally benign, and scalable production of multiple heteroatoms doped HPC with excellent electrochemical performance [98]. Chang et al. [98] developed a facile procedure for fast synthesis of multiple heteroatoms doped HPC by in situ doping of halogenated polymer (dimethyl sulfoxide as S precursor and dimethylformamide for N precursor). The prepared electrodes exhibit excellent specific capacitance (427 F g^{-1} at 1.0 A g^{-1}) in acidic medium and retain ~60% of capacitance at exceedingly high current density (100.0 A g^{-1}) (Table 4). The electrodes also show outstanding electrosorption capacity, cycling stability and wettability. The improvement in the electrical conductivity and specific capacitance of heteroatom doped HPC is attributable to the functionalization effects of the heteroatom(s) on the carbon shell surface [129].

Excellent wettability ensures suitable contact between the electrodes and electrolyte solution, thereby facilitating electrosorption of ions. The study of Xu et al. [137] revealed that phosphorus and nitrogen codoped HPC demonstrated an improved capacitive cell performance. Min et al. [132] also studied cooping of nitrogen and sulfur on porous carbon nanosheet. The produced N, S-CN-600 exhibits excellent electrosorption capacity (55.79 mg g^{-1}) at 1.4 V in 330 mg L^{-1} NaCl solution. Also, N, S-CN-600 electrode demonstrated remarkable reversibility and stability over 20 consecutive charging and discharging cycles.

Furthermore, heteroatom doped HPC enjoys reduced energy loss. Several authors have reported that heteroatom doped HPC exhibits lower charge transfer resistance when compared with the parent HPC behavior [129, 130, 134]. For instance, Ding et al. [129] reported that nitrogen-doped carbon hollow shells (N-CHS) exhibited lower Ohmic resistance (104.8 Ω) than ordinary CHS (376.9 Ω) (Fig. 4a). The Nyquist plots of heteroatom doped HPC are larger slope than 45°, with the line inclining steeply to the imaginary axis, showing faster ion migration and diffusion to the surface of the PCE. This trend reveals that heteroatom doped HPC exhibits remarkable EDL capacitance behavior [131].

The Nyquist plots of EIS in Fig. 4 illustrates how heteroatom doping can influence the resistivity of carbon materials. Heteroatom doping helps to reduce the x-intercept of carbon-based electrodes, indicating minimized bulk resistance (R_s), comprising the resistance of electrolyte solution, inherent resistance of the active surface of the electrode, and the contact resistance at the interface between the current collector electroactive material [101]. The double-layer capacitance (C_{dl}) in parallel with the charge transfer resistance (R_{ct}) at the interface of the electrode/electrolyte is reflected by the small semicircle (quasi-semicircle) in the plots [120, 138]. The decline in the interfacial charge-transfer resistance of the heteroatom doped HPC is ascribed to enhanced hydrophilicity of its surface with increased hydrophilic functional groups.

Table 4 Comparison of the electrosorption performance among various carbon-based electrodes (with and without heteroatom doping) reported in the literature

Sample	Initial NaCl concentration (mg L^{-1})	Working potential (V)	Specific capacitance (F g^{-1})	Sorption capacity (mg/g)	Charge efficiency (%)	Refs.
HPC	500	1.2	66.7	10.27	–	[130]
N-HPC	500	1.2	182.6	13.76	–	[130]
N-HPCA	500	1.2	153	17.9	21	[131]
MMC	1000	1.4	207	20.78	36	[44]
P – C	1000	1.4	150	15.20	–	[44]
K – C	1000	1.4	115	16.63	–	[44]
D – C	1000	1.4	109	9.95	–	[44]
N, S-CN-500[a]	330	1.4	224	–	–	[132]
N, S-CN-600[a]	330	1.4	354.0	55.79	–	[132]
N, S-CN-700[a]	330	1.4	365.0	–	–	[132]
N, S-CN-500[a]	80	1.4	–	14.1	–	[132]
N, S-CN-600[a]	80	1.4	–	21.6	–	[132]
N, S-CN-700[a]	80	1.4	–	21.8	–	[132]
CN-600	80	1.4	–	5.62	–	[132]
N-CN-600	80	1.4	–	9.81	–	[132]
S-CN-600	80	1.4	–	11.4	–	[132]
N-CHS	250	1.6		16.72	–	[129]
CHS	250	1.6		6.61	–	[129]
600[a] -NS-DCM	40	1.6	427	32.3	–	[98]
NSHPC	500	0.5 A g^{-1}	55.56	18.71	–	[99]
N-PHCS	500	1.4	46	12.95		[133]
AC	50	1.2	207.46	1.42	25.44	[134]
AC/SnO_2	50	1.2	233.21	2.19	39.21	[134]
N-AC/SnO_2	50	1.2	408.8	3.42	61.13	[134]
NCPC-900	100	1.2	199.0	11.98	66	[135]
ACs		1.2	52.6	5.2		[136]
NMCs-800[a]	584	1.2	213	20.63		[136]

[a]Cacination temperature; hierarchical porous carbon (HPC); hierarchical porous carbon aerogel (HPCA); N and P codoped micro-/mesoporous carbon (MMC); *D – C* directly calcined pemole peel, *K – C* $KHCO_3$ activated porous carbon using with a carbon to $KHCO_3$ ratio of 1:8, *P – C* $NH_4H_2PO_4$ activated porous carbon using with a carbon to $NH_4H_2PO_4$ ratio of 1:1.24, *NSHPC* Nitrogen and sulfur co-doped three-dimensional (3D) carbon nanosheets, *N-PHCS* nitrogen-doped porous hollow carbon spheres, *NCPCs* nitrogen-doped cluster-like porous carbons, *NMCs* nitrogen-doped mesostructured carbon nanocrystals

Doping of heteroatom like nitrogen can provide additional electron to the HPC substrates readily, meaning that the resistance to the flow of electron is minimized [139]. He et al. [128] reveals that heteroatom doped carbon microsphere remarkably reduces the value of R_s and R_{ct} (Table 5). Therefore, heteroatom doping of porous carbon materials can minimize energy loss and improve their charge transferability, making heteroatom doped carbon promising electrode materials for RGE.

Furthermore, electrode resistance mainly depends on the level of compression of the electrode. An increase in the electrode compression results in a decrease in electrode resistance [140–142]. However, the increase in electrode compression penalizes the porosity of the electrode, thereby limiting electrolyte transport. To attain a balance between these two effects, Park et al. [143] proposed an optimized compression ratio of 20% towards achieving the highest energy efficiency.

5.4 Optimization of Potential of Zero Charge (E_{pzc}) of Carbon Materials

Modification of carbon materials can influence the potential of zero charge (E_{pzc}) and the potential distribution in the capacitive cells, which affect the electrosorption driving force [67, 144]. Wu et al. [100] and Gao et al. [145] proposed that by optimizing the E_{pzc} of PCEs, the cyclic stability, charge efficiency and electrosorption capacity of the electrodes in the capacitive cell can be influenced. The E_{pzc} of PCEs is the potential where no additional ionic charge is

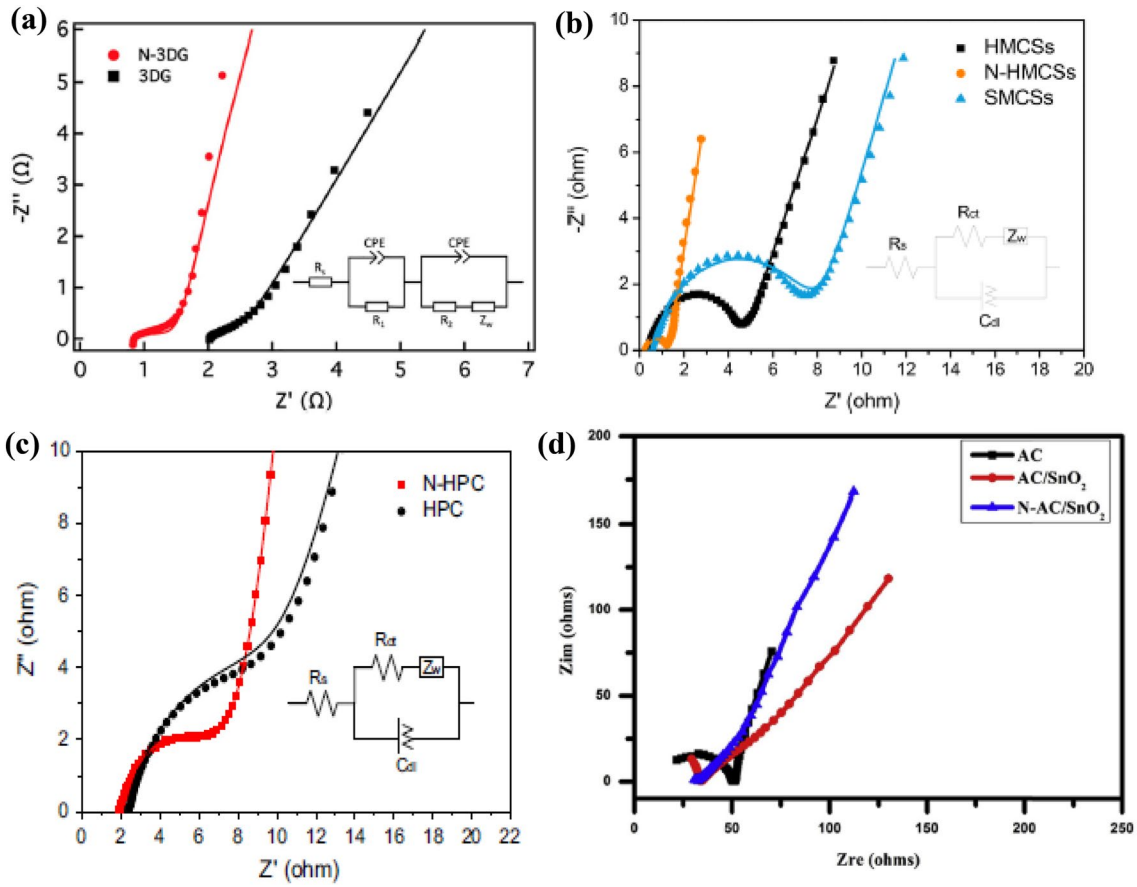

Fig. 4 Nyquist plots of **a** N-CHS (104.8 Ω) and CHS (376.9 Ω) in 1 M NaCl aqueous solution [129]; **b** HMCSs (3.2 Ω), N-HMCSs (1.1 Ω), and SMCSs (7.1 Ω) [120]; **c** HPC (6.14 Ω) and N-HPC (4.58 Ω) [130]; **d** AC, AC/SnO_2,N-AC/SnO_2 [134]. HMCSs: hollow mesoporous carbon spheres; SMCSs: solid mesoporous carbon spheres

Table 5 Resistances and impedance at a different level of heteroatom doping, merging the EIS results and the fitted equivalent circuit [128]

Samples	Rs (Ω)	CPE		Rct (Ω)	W (Ω)
		Yo	N		
CMS-H	9.46	2.93×10^{-5}	0.75	405.7	0.009
CMS-C	5.49	2.66×10^{-6}	0.92	11.9	0.055
CMS-N	3.94	7.50×10^{-6}	0.95	5.3	0.050
CMS-NP	3.67	1.98×10^{-5}	0.96	2.9	0.051

CMS-NP N and P co-doped carbon microsphere

present at the surface of the electrode [146]. If negatively charged functional groups are incorporated to the PECs, the E_{pzc} could shift to a more positive value, while shifting E_{pzc} to a more negative value could be achieved by introducing positively charged functional groups [67, 100]. The E_{pzc} value is quantifiable, and the electrosorption capacity of PECs can be estimated from E_{pzc} and the PEC potential (signified by E). For electrosorption to occurs, the electrode must be polarized away from E_{pzc}. This means that the potential contributing to electrosorption is $|E - E_{pzc}|$ since cations sorption is favored when $E < E_{pzc}$. Anions sorption is favored when $E > E_{pzc}$, while the net ionic charge in the electrode is minimalized when $E = E_{pzc}$ [67, 100]. The use of conventional CDI anode can lead to co-ion expulsion effect triggered by anode oxidation, which negatively influences the sorption capacity and charge efficiency [147]. Co-ion expulsion effect occurs when $E_{pzc} - E_0$ is employed for desorption of previously adsorbed cations when E_{pzc} is positive, and E is polarized from the short circuit potential for ion desorption (E_0) to a more positive value than E_{pzc} [100].

Several authors have modified PCE surface by acid treatment [148–150], metal oxide [138, 151, 152] and sulfonation [90] to introduce negatively charged groups, thereby shifting the E_{pzc} of CDI electrodes positively. Also, some researchers have successfully introduced positively charged species and negatively shift the E_{pzc} of CDI electrodes [100, 153]. Wu, et al. [100] investigated the modification of conventional activated carbon (AC) with quaternized poly (4-vinylpyridine) to synthesized negatively shifted E_{pzc} of CDI electrodes. The E_{pzc} of the as-prepared AC-QPVP electrode

exhibits E_{pzc} of − 0.745 V vs. Ag/AgCl (Fig. 5). AC-QPVP electrode was used together with a nitric acid-modified AC electrode to assemble an asymmetric CDI cell. The electrode demonstrated a remarkable eV-CDI and i-CDI performance with working potential window up to 1.4 V (9.6 mg/g) and 1.2/− 1.2 V (20.6 mg/g) for i-CDI and eV-CDI. The study of Ma et al. [154] also affirm that by optimizing the E_{pzc}, the ion electrosorption behavior of the electrodes in CDI system can be enhanced using asymmetric cell configuration.

5.5 Optimization of Cell Configuration

The electrosorption performance of the composite electrodes can be maximized by a rational configuration of electrodes in the capacitive cell, either symmetric or asymmetric with a careful selection of anode and cathode material [155–157]. The study of Omosebi et al. [150] using a combination of oxidized Zorflex (ZX) and pristine ZX electrodes revealed that the highest electro-sorption capacity (17 mg NaCl/g ZX) was observed for the capacitive cell configuration comprising oxidized ZX as the cathode and pristine ZX as the anode. Liu et al. [138] comparatively studied the desalination performance of two different CDI cell architecture, + ZnO/AC||AC (AC as cathode and ZnO/AC as the anode), and − ZnO/AC||AC (ZnO/AC as cathode and AC as the anode). They observed that − ZnO/AC||AC capacitor

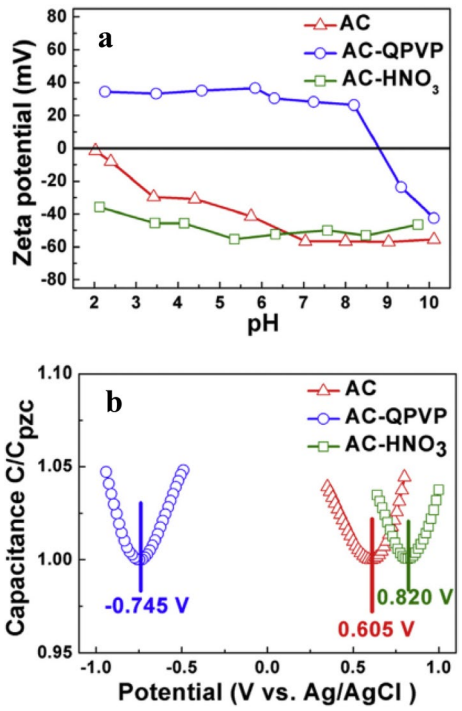

Fig. 5 **a** Zeta potential, and **b** Normalized differential capacitance curves of the electrodes prepared from AC, AC-HNO_3 and AC-QPVP [100]

is more durable and exhibited a better desalination performance (9.4 mg/g) than + ZnO/AC||AC. Ma et al. [26] studied the optimization of CDI configuration using electrodes prepared from CNT/PPy composites doped with dodecylbenzene sulfonate (DBS^-) and chloride (Cl^-). They assembled seven different types of asymmetric and symmetric CDI cells. They reported that the electrosorption performance for CDI cells largely depends on the E_{pzc} of the electrodes and the distribution of the cell's potential (Table 6).

In a recent work of Gao et al. [158], a carbon material was oxidized to improve its negative chemical surface charge. The as-prepared material was used to design a CDI cell with symmetric architecture and different E_{pzc} versus E_0 in a potential distribution. Their study unravelled a novel analytical approach for estimation of E_{pzc} and potential distribution diagram by leveraging on modified Donnan (mD) model with chemical surface charge. In mD model, the chemical surface charge (σ_{chem}) values are measured by examining the steady-state value of effluent pH with and without the electrode pairs in the flow cell (Eqs. 11 and 12). Where m is the electrode weight, v_{mic} is the micropore volume of the electrode and V_{sol} is the volume of the solution. This novel approach boosts the efficiency of constant-voltage CDI with symmetric configuration since the as-prepared carbon electrode exhibits a net σ_{chem} of zero or equal negative ($\sigma_{chem,-}$) and positive ($\sigma_{chem,+}$) value of σ_{chem}. The result of mapping E_{pzc} and E_0 in a potential distribution diagram reveals that the co-ion expulsion effect associated with conventional CDI anode at the intermediate charge storage stage was suppressed. Therefore, the performance of CDI cells can be interpreted and predicted, having known the values of charge balances together with the potential distribution.

$$\sigma_{chem,+} = (10^{(pH-14)}V_{sol})/(V_{mic}m) \tag{11}$$

$$\sigma_{chem,-} = (10^{(-pH)}V_{sol})/(V_{mic}m) \tag{12}$$

5.6 Process Intensification

In CDI process, the sustenance of EDLs established within PCEs when an electrical potential is applied significantly depends on the capture of charged species. The process can be improved by the functionalizing the fixed charged groups of the porous electrodes of enhanced CDI (ECDI) with constant chemical charge [159]. Since conventional carbon materials are certainly known to permit parasitic Faradaic reaction, it is essential to replace conventional carbon materials with faradaic electrode materials, which can store ions through faradaic redox reactions 160. Faradaic electrodes have attracted the attention of several scholars due to their high capacity, selective ion electrosorption and low energy loss.

Table 6 Performance of capacitive cells based on cell configuration

Anode/(E_{pzc})	Cathode/(E_{pzc})	Type	Solution	Working potential (V)	Sorption capacity (mg/g)	Charge efficiency (%)	Refs.
CNT/(0 V vs. SCE)	CNT/(0 V vs. SCE)	CDI	500 ppm NaCl	1.2	6.61	24.4	[26]
CNT/PPy-Cl/(−0.1 V vs. SCE)	CNT/(0 V vs. SCE)	CDI	500 ppm NaCl	1.2	19.9	44.5	[26]
CNT/(0 V vs. SCE)	CNT/PPy-Cl/(−0.1 V vs. SCE)	CDI	500 ppm NaCl	1.2	11.9	30.9	[26]
CNT/(0 V vs. SCE)	CNT/PPy-DBS/(0.4 V vs. SCE)	CDI	500 ppm NaCl	1.2	20.7	45.8	[26]
CNT/PPy-DBS/(0.4 V vs. SCE)	CNT/(0 V vs. SCE)	CDI	500 ppm NaCl	1.2	13.9	31.4	[26]
CNT/PPy-DBS/(0.4 V vs. SCE)	CNT/PPy-Cl/(−0.1 V vs. SCE)	CDI	500 ppm NaCl	1.2	17.50	34.2	[26]
CNT/PPy-Cl/(−0.1 V vs. SCE)	CNT/PPy-DBS/(0.4 V vs. SCE)	CDI	500 ppm NaCl	1.2	35.46	58.9	[26]
pristine ZX/(−0.2 V vs. SCE)	pristine ZX(−0.2 V vs. SCE)	MCDI	5 mM NaCl	1.2	7.71	92.6	[150]
pristine ZX(−0.2 V vs. SCE)	oxidized ZX/(0.2 V vs. SCE)	MCDI	5 mM NaCl	1.2	17.3	132	[150]
oxidized ZX/ (0.2 V vs. SCE)	pristine ZX(−0.2 V vs. SCE)	MCDI	5 mM NaCl	1.2	4.72	62.4	[150]
oxidized ZX/(0.2 V vs. SCE)	oxidized ZX/(0.2 V vs. SCE)	MCDI	5 mM NaCl	1.2	11.3	109	[150]
Untreated carbon cloth (−0.22 V vs. SCE)	Untreated carbon cloth (−0.22 V vs. SCE)	CDI	9 mM NaCl	0.8	7.5	~50	[158]
3 times oxidized carbon cloth (0 V vs. SCE)	3 times oxidized carbon cloth (0 V vs. SCE)	CDI	9 mM NaCl	0.8	12.5	~75	[158]
7 times oxidized carbon cloth (0.36 V vs. SCE)	7 times oxidized carbon cloth (0.36 V vs. SCE)	CDI	9 mM NaCl	0.8	5.6	~45	[158]

Recently, several scientists have demonstrated that by functionalizing the carbon matrix with redox polymers, the energy storage capacity of the electrodes can be improved [159]. The improvement was attributed to modulation of the charge on the electrodes via Faradaic reactions when subjected to different cell voltages in a capacitive process that could be referred to as "Faradaic CDI" (FaCDI) [161]. FaCDI electrodes are redox-active materials that combine a double layer charging process with Faradaic reactions, which induced the synergistic formation of charged species. These charged species make the adsorption capacity of FaCDI electrodes higher than in the conventional CDI and ECDI (Fig. 6) since the electrostatic interactions of ions with Faradaically-induced charges added to the ions incorporated within the EDLs are generated at the surface of the electrodes. The report of He et al. [159] reveals that redox-active FaCDI electrodes offer a novel approach for enhancement of CDI cells performance, as well as energy storage capacity. FaCDI electrodes can be combined with other species to produce hybrid materials that propel further study towards understanding the mechanisms of ion adsorption.

Hybrid capacitive deionization (HCDI) involves a combination of a redox-active electrode and a capacitive carbon electrode in a single cell to enable higher ion sorption capacity than capacitive cells that contains two carbon electrodes. Byles et al. [31] investigated the electrochemical response of manganese oxide nanowires in combination with four different tunnel crystal structures as faradaic electrodes in HCDI system. The ion electrosorption behavior of the nanowires was studied in NaCl solution,

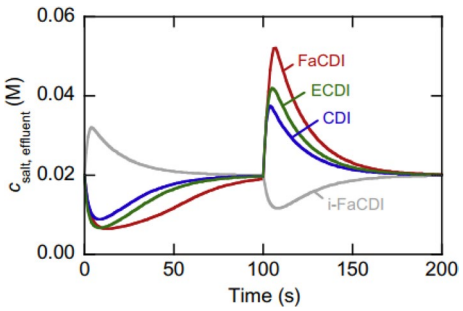

Fig. 6 Comparison of effluent salt concentrations in the adsorption/desorption cycle (V_{ch}=0:6 V for enhanced FaCDI ($\Delta\phi^{\emptyset}_{S_{eq,A}}$ = 0.1 V), classical CDI and enhanced CDI; V_{ch}=−0.45 V for inverted FaCDI ($\Delta\phi^{\emptyset}_{S_{eq,A}}$ = −0.3 V), V_{disch}=0 V for all curves) [159]

which is commonly used in laboratory experiments. $MgCl_2$ and KCl media were also examined to provide a better insight into the behavior of these materials for desalination of brackish water, containing multiple cation species. The reported that the manganese oxide electrodes exhibits excellent stability in repeated electrosorption and release cycles. The compositional analysis of the electrodes revealed that the electrosorption is achieved via intercalation of ions into the structural tunnels and surface redox reactions.

6 Conclusion

The future of reactive gas electrosorption (RGE) technology is bright, leveraging on the extensively studied capacitive cell techniques in wastewater treatment. RGE involves mixing of air stream containing a low concentration of CO_2 with a stream containing high CO_2 concentration in water or alkaline aqueous electrolyte. However, this concept is faced with the challenges of designs specific for CO_2-electrolyte, and porous carbon electrodes (PCEs) limitations, which engender low performance and energy loss. The drawback relating to the electrode could be solved using heteroatom doped traditional carbon materials and composite carbon-based materials, which has been successfully used in capacitive cells designed for desalination. This modification helps to improve the hydrophilicity, and consequently improve electrode wettability, suppresses faradaic reaction and the co-ion repulsion effect. This improvement enhances the charge efficiency, sorption capacity durability of electrodes and reduces the energy loss in RGE.

Since the electrosorption performance of a capacitive cell largely depends on the potential of zero charge (E_{pzc}) of the electrodes and the distribution of the cell's potential, and the fact that the E_{pzc} of porous carbon materials is amenable, the capacitive cell configuration can be optimized for enhanced performance. Moreover, intensification of the membrane capacitive deionization (MCDI) process to obtain variances like enhanced MCDI, Faradaic MCDI, and Hybrid capacitive deionization (HCDI) is also a promising approach for improvement of the capacitive cell design in RGE. This intensification could improve the electrosorption capacity and minimize the negative effect of faradaic reaction.

Moreover, the use of amine blend like Piperazine (PZ)-based as an alternative, which is less susceptible to degradation, thereby boosting CO_2 dissolution. PZ and its derivatives carry a better cyclic capacity and dissolution rate than the benchmark monoethanolamine (MEA). However, amines show a proper CO_2 loading, but they have a slow dissolution rate. The rate of dissolution of amines may be increased by adding PZ as a promoter. This review will help to promote the development of RGE technologies based on capacitive cell, towards providing sustainable, cost-effective means for CO_2 capture and utilization.

Acknowledgements The authors acknowledge the Fundamental Research Grant Scheme (FRGS) from the Ministry of Education (Department of Higher Education), Malaysia for funding this work through Project No. "FP046-2017A".

Author contributions HUF contributed in the conceptualization and section 3 (Reactive Gas Electrosorption (RGE)) of the manuscript.

References

1. Porada, S., et al. (2014). Carbon flow electrodes for continuous operation of capacitive deionization and capacitive mixing energy generation. *Journal of Materials Chemistry A, 2*, 9313–9321.
2. Paz-Garcia, J. M., Dykstra, J., Biesheuvel, P., & Hamelers, H. (2015). Energy from CO_2 using capacitive electrodes–a model for energy extraction cycles. *Journal of Colloid and Interface Science, 442*, 103–109.
3. Hamelers, H., Schaetzle, O., Paz-García, J., Biesheuvel, P., & Buisman, C. (2013). Harvesting energy from CO_2 emissions. *Environmental Science & Technology Letters, 1*, 31–35.
4. Logan, B. E., & Elimelech, M. (2012). Membrane-based processes for sustainable power generation using water. *Nature, 488*, 313.
5. Post, J. W., et al. (2007). Salinity-gradient power: Evaluation of pressure-retarded osmosis and reverse electrodialysis. *Journal of membrane science, 288*, 218–230.
6. Pattle, R. (1954). Production of electric power by mixing fresh and salt water in the hydroelectric pile. *Nature, 174*, 660.
7. Brogioli, D., et al. (2012). Exploiting the spontaneous potential of the electrodes used in the capacitive mixing technique for the extraction of energy from salinity difference. *Energy & Environmental Science, 5*, 9870–9880.
8. Liu, F., et al. (2012). Effect of additional charging and current density on the performance of Capacitive energy extraction based on Donnan Potential. *Energy & Environmental Science, 5*, 8642–8650.
9. Rica, R. A., et al. (2013). Electro-diffusion of ions in porous electrodes for capacitive extraction of renewable energy from salinity differences. *Electrochimica Acta, 92*, 304–314.
10. Brogioli, D. (2009). Extracting renewable energy from a salinity difference using a capacitor. *Physical Review Letters, 103*, 058501.
11. Porada, S., et al. (2012). Water desalination using capacitive deionization with microporous carbon electrodes. *ACS Applied Materials & Interfaces, 4*, 1194–1199.
12. Porada, S., Zhao, R., Van Der Wal, A., Presser, V., & Biesheuvel, P. (2013). Review on the science and technology of water desalination by capacitive deionization. *Progress in Materials Science, 58*, 1388–1442.
13. Zhao, R., Biesheuvel, P., & Van der Wal, A. (2012). Energy consumption and constant current operation in membrane capacitive deionization. *Energy & Environmental Science, 5*, 9520–9527.
14. Merlet, C., et al. (2012). On the molecular origin of supercapacitance in nanoporous carbon electrodes. *Nature Materials, 11*, 306.
15. Kondrat, S., Perez, C., Presser, V., Gogotsi, Y., & Kornyshev, A. (2012). Effect of pore size and its dispersity on the energy storage in nanoporous supercapacitors. *Energy & Environmental Science, 5*, 6474–6479.
16. Jande, Y., Asif, M., Shim, S., & Kim, W.-S. (2014). Energy minimization in monoethanolamine-based CO_2 capture using capacitive deionization. *International Journal of Energy Research, 38*, 1531–1540.
17. Paz-Garcia, J. M., Schaetzle, O., Biesheuvel, P., & Hamelers, H. (2014). Energy from CO_2 using capacitive electrodes–Theoretical outline and calculation of open circuit voltage. *Journal of Colloid and Interface Science, 418*, 200–207.
18. Chi, S., & Rochelle, G. T. (2002). Oxidative degradation of monoethanolamine. *Industrial & Engineering Chemistry Research, 41*, 4178–4186.
19. Bijmans, M., et al. (2012). Capmix-deploying capacitors for salt gradient power extraction. *Energy Procedia, 20*, 108–115.

20. Dykstra, J., Keesman, K., Biesheuvel, P., & Van der Wal, A. (2017). Theory of pH changes in water desalination by capacitive deionization. *Water Research, 119*, 178–186.
21. Jiménez, M., Fernandez, M., Ahualli, S., Iglesias, G., & Delgado, A. (2013). Predictions of the maximum energy extracted from salinity exchange inside porous electrodes. *Journal of Colloid and Interface Science, 402*, 340–349.
22. García-Quismondo, E., Santos, C., Lado, J., Palma, J. S., & Anderson, M. A. (2013). Optimizing the energy efficiency of capacitive deionization reactors working under real-world conditions. *Environmental Science & Technology, 47*, 11866–11872.
23. Teng, H., Chang, Y.-J., & Hsieh, C.-T. (2001). Performance of electric double-layer capacitors using carbons prepared from phenol–formaldehyde resins by KOH etching. *Carbon, 39*, 1981–1987.
24. Zhang, L. L., Gu, Y., & Zhao, X. (2013). Advanced porous carbon electrodes for electrochemical capacitors. *Journal of Materials Chemistry A, 1*, 9395–9408.
25. Anderson, M. A., Cudero, A. L., & Palma, J. (2010). Capacitive deionization as an electrochemical means of saving energy and delivering clean water. Comparison to present desalination practices: will it compete? *Electrochimica Acta, 55*, 3845–3856.
26. Ma, J., Wang, L., & Yu, F. (2018). Water-enhanced performance in capacitive deionization for desalination based on graphene gel as electrode material. *Electrochimica Acta, 263*, 40–46.
27. Zhang, T., Zhao, H., Huang, X., & Wen, G. (2016). Li-ion doped graphene/carbon nanofiber porous architectures for electrochemical capacitive desalination. *Desalination, 379*, 118–125.
28. Suss, M., et al. (2015). Water desalination via capacitive deionization: What is it and what can we expect from it? *Energy & Environmental Science, 8*, 2296–2319.
29. Xu, X., Sun, Z., Chua, D. H., & Pan, L. (2015). Novel nitrogen doped graphene sponge with ultrahigh capacitive deionization performance. *Scientific Reports, 5*, 11225.
30. Lee, J., Kim, S., Kim, C., & Yoon, J. (2014). Hybrid capacitive deionization to enhance the desalination performance of capacitive techniques. *Energy & Environmental Science, 7*, 3683–3689.
31. Byles, B. W., Cullen, D. A., More, K. L., & Pomerantseva, E. (2018). Tunnel structured manganese oxide nanowires as redox active electrodes for hybrid capacitive deionization. *Nano Energy, 44*, 476–488.
32. 32Legrand, L. (2018) *Reactive Gas Electrosorption (RGE): Electricity production/CO_2 capture*, https://www.wetsus.nl/includes/downloadFile.asp?id=YzkxTmpNeE9BPT1iMGU%3D&date=c91b0e.
33. Legrand, L., Schaetzle, O., Hamelers, H., de Kler, R. & Buisman, C. Reactive gas electrosorption: novel, clean and energy efficient CO_2 capture concept. In *9th Trondheim conference on carbon capture, transport and storage*. http://programme.exordo.com/tccs-9/delegates/presentation/53/.
34. Biesheuvel, P., Porada, S., Levi, M., & Bazant, M. Z. (2014). Attractive forces in microporous carbon electrodes for capacitive deionization. *Journal of Solid State Electrochemistry, 18*, 1365–1376.
35. Chandan, P. A., Remias, J. E., Neathery, J. K., & Liu, K. (2013). Morpholine nitrosation to better understand potential solvent based CO2 capture process reactions. *Environmental Science & Technology, 47*, 5481–5487.
36. Huang, Q., et al. (2013). Impact of flue gas contaminants on monoethanolamine thermal degradation. *Industrial & Engineering Chemistry Research, 53*, 553–563.
37. Saeed, I. M., et al. (2018). Opportunities and challenges in the development of monoethanolamine and its blends for post-combustion CO_2 capture. *International Journal of Greenhouse Gas Control, 79*, 212–233. https://doi.org/10.1016/j.ijggc.2018.11.002.
38. Sexton, A. J., & Rochelle, G. T. (2010). Reaction products from the oxidative degradation of monoethanolamine. *Industrial & Engineering Chemistry Research, 50*, 667–673.
39. Chandan, P., Richburg, L., Bhatnagar, S., Remias, J. E., & Liu, K. (2014). Impact of fly ash on monoethanolamine degradation during CO_2 capture. *International Journal of Greenhouse Gas Control, 25*, 102–108.
40. Mangalapally, H. P., & Hasse, H. (2011). Pilot plant experiments for post combustion carbon dioxide capture by reactive absorption with novel solvents. *Energy Procedia, 4*, 1–8.
41. Moser, P., Schmidt, S., & Stahl, K. (2011). Investigation of trace elements in the inlet and outlet streams of a MEA-based post-combustion capture process results from the test programme at the Niederaussem pilot plant. *Energy Procedia, 4*, 473–479.
42. Bedell, S. A. (2009). Oxidative degradation mechanisms for amines in flue gas capture. *Energy Procedia, 1*, 771–778.
43. Sexton, A. J., & Rochelle, G. T. (2009). Catalysts and inhibitors for oxidative degradation of monoethanolamine. *International Journal of Greenhouse Gas Control, 3*, 704–711.
44. Dong, Q., Wang, G., Wu, T., Peng, S., & Qiu, J. (2015). Enhancing capacitive deionization performance of electrospun activated carbon nanofibers by coupling with carbon nanotubes. *Journal of Colloid and Interface Science, 446*, 373–378.
45. Wang, G., et al. (2012). Hierarchical activated carbon nanofiber webs with tuned structure fabricated by electrospinning for capacitive deionization. *Journal of Materials Chemistry, 22*, 21819–21823.
46. Li, Y., Jiang, Y., Wang, T.-J., Zhang, C., & Wang, H. (2017). Performance of fluoride electrosorption using micropore-dominant activated carbon as an electrode. *Separation and Purification Technology, 172*, 415–421.
47. Choi, J.-H. (2010). Fabrication of a carbon electrode using activated carbon powder and application to the capacitive deionization process. *Separation and Purification Technology, 70*, 362–366.
48. Jung, H.-H., Hwang, S.-W., Hyun, S.-H., Lee, K.-H., & Kim, G.-T. (2007). Capacitive deionization characteristics of nanostructured carbon aerogel electrodes synthesized via ambient drying. *Desalination, 216*, 377–385.
49. Nugrahenny, A. T. U., et al. (2014). Preparation and application of reduced graphene oxide as the conductive material for capacitive deionization. *Carbon Letters, 15*, 38–44.
50. Xing, Z., et al. (2015). Reducing CO_2 to dense nanoporous graphene by Mg/Zn for high power electrochemical capacitors. *Nano Energy, 11*, 600–610.
51. Wang, Y., Han, X., Wang, R., Xu, S., & Wang, J. (2015). Preparation optimization on the coating-type polypyrrole/carbon nanotube composite electrode for capacitive deionization. *Electrochimica Acta, 182*, 81–88.
52. Hou, C.-H., Liu, N.-L., Hsu, H.-L., & Den, W. (2014). Development of multi-walled carbon nanotube/poly (vinyl alcohol) composite as electrode for capacitive deionization. *Separation and Purification Technology, 130*, 7–14.
53. Tkachev, S., Buslaeva, E. Y., & Gubin, S. (2011). Graphene: A novel carbon nanomaterial. *Inorganic Materials, 47*, 1–10.
54. Wang, Z., et al. (2012). Effective desalination by capacitive deionization with functional graphene nanocomposite as novel electrode material. *Desalination, 299*, 96–102.
55. Li, H., et al. (2011). A comparative study on electrosorptive behavior of carbon nanotubes and graphene for capacitive deionization. *Journal of Electroanalytical Chemistry, 653*, 40–44.
56. Xu, X., et al. (2015). Rational design and fabrication of graphene/carbon nanotubes hybrid sponge for high-performance

capacitive deionization. *Journal of Materials Chemistry A, 3*, 13418–13425.
57. Wang, H., et al. (2013). Three-dimensional macroporous graphene architectures as high performance electrodes for capacitive deionization. *Journal of Materials Chemistry A, 1*, 11778–11789.
58. Oladunni, J., et al. (2018). A comprehensive review on recently developed carbon based nanocomposites for capacitive deionization: from theory to practice. *Separation and Purification Technology, 207*, 291–320.
59. Min, B. H., Choi, J.-H., & Jung, K. Y. (2018). Improved capacitive deionization of sulfonated carbon/titania hybrid electrode. *Electrochimica Acta, 270*, 543–551.
60. Liu, P., et al. (2016). Grafting sulfonic and amine functional groups on 3D graphene for improved capacitive deionization. *Journal of Materials Chemistry A, 4*, 5303–5313.
61. Zhang, C., He, D., Ma, J., Tang, W., & Waite, T. D. (2018). Faradaic reactions in capacitive deionization (CDI)-problems and possibilities: A review. *Water Research, 128*, 314–330.
62. Lee, J.-H., Bae, W.-S., & Choi, J.-H. (2010). Electrode reactions and adsorption/desorption performance related to the applied potential in a capacitive deionization process. *Desalination, 258*, 159–163.
63. Maass, S., Finsterwalder, F., Frank, G., Hartmann, R., & Merten, C. (2008). Carbon support oxidation in PEM fuel cell cathodes. *Journal of Power Sources, 176*, 444–451.
64. Oh, H.-S., et al. (2008). On-line mass spectrometry study of carbon corrosion in polymer electrolyte membrane fuel cells. *Electrochemistry Communications, 10*, 1048–1051.
65. Holubowitch, N., Omosebi, A., Gao, X., Landon, J., & Liu, K. (2017). Quasi-steady-state polarization reveals the interplay of capacitive and faradaic processes in capacitive deionization. *ChemElectroChem, 4*, 2404–2413.
66. Haro, M., Rasines, G., Macias, C., & Ania, C. (2011). Stability of a carbon gel electrode when used for the electro-assisted removal of ions from brackish water. *Carbon, 49*, 3723–3730.
67. Cohen, I., Avraham, E., Bouhadana, Y., Soffer, A., & Aurbach, D. (2015). The effect of the flow-regime, reversal of polarization, and oxygen on the long term stability in capacitive de-ionization processes. *Electrochimica Acta, 153*, 106–114.
68. Bouhadana, Y., Ben-Tzion, M., Soffer, A., & Aurbach, D. (2011). A control system for operating and investigating reactors: the demonstration of parasitic reactions in the water desalination by capacitive de-ionization. *Desalination, 268*, 253–261.
69. Cohen, I., Avraham, E., Bouhadana, Y., Soffer, A., & Aurbach, D. (2013). Long term stability of capacitive de-ionization processes for water desalination: the challenge of positive electrodes corrosion. *Electrochimica Acta, 106*, 91–100.
70. Porada, S., et al. (2013). Direct prediction of the desalination performance of porous carbon electrodes for capacitive deionization. *Energy & Environmental Science, 6*, 3700–3712.
71. Duan, F., Du, X., Li, Y., Cao, H., & Zhang, Y. (2015). Desalination stability of capacitive deionization using ordered mesoporous carbon: effect of oxygen-containing surface groups and pore properties. *Desalination, 376*, 17–24.
72. Gao, X., Omosebi, A., Landon, J., & Liu, K. (2014). Dependence of the capacitive deionization performance on potential of zero charge shifting of carbon xerogel electrodes during long-term operation. *Journal of The Electrochemical Society, 161*, E159–E166.
73. Hemmatifar, A., Palko, J. W., Stadermann, M., & Santiago, J. G. (2016). Energy breakdown in capacitive deionization. *Water Research, 104*, 303–311.
74. Qu, Y., et al. (2016). Energy consumption analysis of constant voltage and constant current operations in capacitive deionization. *Desalination, 400*, 18–24.
75. Arstad, B., Blom, R., & Swang, O. (2007). CO_2 absorption in aqueous solutions of alkanolamines: Mechanistic insight from quantum chemical calculations. *The Journal of Physical Chemistry A, 111*, 1222–1228.
76. Yang, L., et al. (2011). Boron-doped carbon nanotubes as metal-free electrocatalysts for the oxygen reduction reaction. *Angewandte Chemie International Edition, 50*, 7132–7135.
77. Chen, X., & Rochelle, G. T. (2011). Aqueous piperazine derivatives for CO2 capture: Accurate screening by a wetted wall column. *Chemical Engineering Research and Design, 89*, 1693–1710.
78. Léonard, G. (2012). *Degradation inhibitors and metal additives: impact on solvent degradation*. Laborelec. https://orbi.uliege.be/handle/2268/177360.
79. Alaba, P. A., Adedigba, S. A., Olupinla, S. F., Agboola, O., & Sanni, S. E. (2020). Unveiling corrosion behavior of pipeline steels in CO_2-containing oilfield produced water: towards combating the corrosion curse. *Critical Reviews in Solid State and Materials Sciences*, *45*(3), 239–260.
80. Blachly, C., & Ravner, H. (1966). Stabilization of monoethanolamine solutions in carbon dioxide scrubbers. *Journal of Chemical and Engineering Data, 11*, 401–403.
81. Léonard, G., Voice, A., Toye, D., & Heyen, G. (2014). Influence of dissolved metals and oxidative degradation inhibitors on the oxidative and thermal degradation of monoethanolamine in postcombustion CO_2 capture. *Industrial & Engineering Chemistry Research*, *53*(47), 18121–18129.
82. Lawal, O., Bello, A., & Idem, R. (2005). The role of methyl diethanolamine (MDEA) in preventing the oxidative degradation of CO_2 loaded and concentrated aqueous monoethanolamine (MEA)—MDEA blends during CO_2 absorption from flue gases. *Industrial & Engineering chemistry research, 44*, 1874–1896.
83. Goff, G. S., & Rochelle, G. T. (2006). Oxidation inhibitors for copper and iron catalyzed degradation of monoethanolamine in CO_2 capture processes. *Industrial & Engineering Chemistry Research, 45*, 2513–2521.
84. Léonard, G., Voice, A., Toye, D., & Heyen, G. (2014). Influence of dissolved metals and oxidative degradation inhibitors on the oxidative and thermal degradation of monoethanolamine in postcombustion CO_2 capture. *Industrial & Engineering Chemistry Research, 53*, 18121–18129.
85. Sexton, A. J., & Rochelle, G. T. (2009). Catalysts and inhibitors for MEA oxidation. *Energy Procedia, 1*, 1179–1185.
86. Carrette, P. L., & Delfort, B. (2014). U.S. Patent No. 8,765,088. Washington, DC: U.S. Patent and Trademark Office.
87. Lei, H., et al. (2015). Graphene-like carbon nanosheets prepared by a Fe-catalyzed glucose-blowing method for capacitive deionization. *Journal of Materials Chemistry A, 3*, 5934–5941.
88. Yang, J., & Zou, L. (2014). Recycle of calcium waste into mesoporous carbons as sustainable electrode materials for capacitive deionization. *Microporous and Mesoporous Materials, 183*, 91–98.
89. Sharma, K., et al. (2015). Transport of ions in mesoporous carbon electrodes during capacitive deionization of high-salinity solutions. *Langmuir, 31*, 1038–1047.
90. Qian, B., et al. (2015). Sulfonated graphene as cation-selective coating: A new strategy for high-performance membrane capacitive deionization. *Advanced Materials Interfaces, 2*, 1500372.
91. Liu, Y., et al. (2015). Nitrogen-doped porous carbon spheres for highly efficient capacitive deionization. *Electrochimica Acta, 158*, 403–409.
92. Hou, C.-H., Liu, N.-L., & Hsi, H.-C. (2015). Highly porous activated carbons from resource-recovered Leucaena leucocephala

wood as capacitive deionization electrodes. *Chemosphere, 141*, 71–79.
93. Porada, S., et al. (2015). Capacitive deionization using biomass-based microporous salt-templated heteroatom-doped carbons. *Chemsuschem, 8*, 1867–1874.
94. Li, H., et al. (2015). The study of capacitive deionization behavior of a carbon nanotube electrode from the perspective of charge efficiency. *Water Science and Technology, 71*, 83–88.
95. Wang, L., et al. (2011). Capacitive deionization of NaCl solutions using carbon nanotube sponge electrodes. *Journal of Materials Chemistry, 21*, 18295–18299.
96. Kumar, R., et al. (2016). Carbon aerogels through organo-inorganic co-assembly and their application in water desalination by capacitive deionization. *Carbon, 99*, 375–383.
97. Rasines, G., et al. (2015). N-doped monolithic carbon aerogel electrodes with optimized features for the electrosorption of ions. *Carbon, 83*, 262–274.
98. Chang, Y., et al. (2017). Polymer dehalogenation-enabled fast fabrication of N, S-codoped carbon materials for superior supercapacitor and deionization applications. *ACS Applied Materials & Interfaces, 9*, 29753–29759.
99. Huang, Y., et al. (2019). Mycelial pellet-derived heteroatom-doped carbon nanosheets with a three-dimensional hierarchical porous structure for efficient capacitive deionization. *Environmental Science: Nano, 6*, 1430–1442.
100. Wu, T., et al. (2016). Surface-treated carbon electrodes with modified potential of zero charge for capacitive deionization. *Water Research, 93*, 30–37.
101. Gao, T., Zhou, F., Ma, W., & Li, H. (2018). Metal-organic-framework derived carbon polyhedron and carbon nanotube hybrids as electrode for electrochemical supercapacitor and capacitive deionization. *Electrochimica Acta, 263*, 85–93.
102. Xu, X., Wang, M., Liu, Y., Lu, T., & Pan, L. (2016). Metal–organic framework-engaged formation of a hierarchical hybrid with carbon nanotube inserted porous carbon polyhedra for highly efficient capacitive deionization. *Journal of Materials Chemistry A, 4*, 5467–5473.
103. Wu, T., et al. (2018). Highly stable hybrid capacitive deionization with a MnO_2 anode and a positively charged cathode. *Environmental Science & Technology Letters, 5*, 98–102.
104. Yasin, A. S., Obaid, M., Mohamed, I. M., Yousef, A., & Barakat, N. A. (2017). ZrO_2 nanofibers/activated carbon composite as a novel and effective electrode material for the enhancement of capacitive deionization performance. *Rsc Advances, 7*, 4616–4626.
105. Yasin, A. S., Mohamed, I. M., Mousa, H. M., Park, C. H., & Kim, C. S. (2018). Facile synthesis of TiO_2/ZrO_2 nanofibers/nitrogen co-doped activated carbon to enhance the desalination and bacterial inactivation via capacitive deionization. *Scientific Reports, 8*, 541.
106. Iorio, M., De Martino, A., Violante, A., Pigna, M., & Capasso, R. (2010). Synthesis, characterization, and sorption capacity of layered double hydroxides and their complexes with polymerin. *Journal of Agricultural and Food Chemistry, 58*, 5523–5530.
107. Poznyak, S., et al. (2009). Novel inorganic host layered double hydroxides intercalated with guest organic inhibitors for anticorrosion applications. *ACS Applied Materials & Interfaces, 1*, 2353–2362.
108. Lv, L., He, J., Wei, M., Evans, D., & Duan, X. (2006). Uptake of chloride ion from aqueous solution by calcined layered double hydroxides: Equilibrium and kinetic studies. *Water Research, 40*, 735–743.
109. Lv, L., He, J., Wei, M., Evans, D., & Duan, X. (2006). Factors influencing the removal of fluoride from aqueous solution by calcined Mg–Al–CO_3 layered double hydroxides. *Journal of Hazardous Materials, 133*, 119–128.
110. Gao, Z., et al. (2011). Graphene nanosheet/Ni^{2+}/Al^{3+} layered double-hydroxide composite as a novel electrode for a supercapacitor. *Chemistry of Materials, 23*, 3509–3516.
111. Ren, Q., et al. (2018). Calcined MgAl-layered double hydroxide/graphene hybrids for capacitive deionization. *Industrial & Engineering Chemistry Research, 57*, 6417–6425.
112. El-Deen, A. G., et al. (2015). TiO_2 nanorod-intercalated reduced graphene oxide as high performance electrode material for membrane capacitive deionization. *Desalination, 361*, 53–64.
113. Yin, H., et al. (2013). Three-dimensional graphene/metal oxide nanoparticle hybrids for high-performance capacitive deionization of saline water. *Advanced Materials, 25*, 6270–6276.
114. Liu, R., et al. (2016). Shrimp-shell derived carbon nanodots as carbon and nitrogen sources to fabricate three-dimensional N-doped porous carbon electrocatalysts for the oxygen reduction reaction. *Physical Chemistry Chemical Physics, 18*, 4095–4101.
115. Bayatsarmadi, B., Zheng, Y., Jaroniec, M., & Qiao, S. Z. (2015). Soft-templating synthesis of N-doped mesoporous carbon nanospheres for enhanced oxygen reduction reaction. *Chemistry–An Asian Journal, 10*, 1546–1553.
116. Yang, W., Yue, X., Liu, X., Zhai, J., & Jia, J. (2015). IL-derived N, S co-doped ordered mesoporous carbon for high-performance oxygen reduction. *Nanoscale, 7*, 11956–11961.
117. Hoyt, R. A., Remillard, E. M., Cubuk, E. D., Vecitis, C. D., & Kaxiras, E. (2016). Polyiodide-doped graphene. *The Journal of Physical Chemistry C, 121*, 609–615.
118. Alaba, P. A., Lee, C. S., Abnisa, F., Aroua, M. K., Cognet, P., Pérès, Y., et al. (2020). A review of recent progress on electrocatalysts toward efficient glycerol electrooxidation. *Reviews in Chemical Engineering*. https://doi.org/10.1515/revce-2019-0013.
119. Alaba, P. A., et al. (2020). Investigating the electrocatalytic oxidation of glycerol on simultaneous nitrogen-and fluorine-doped on activated carbon black composite. *Diamond and Related Materials, 101*, 107626.
120. Li, Y., et al. (2017). Nitrogen-doped hollow mesoporous carbon spheres for efficient water desalination by capacitive deionization. *ACS Sustainable Chemistry & Engineering, 5*, 6635–6644.
121. Lin, T., et al. (2015). Nitrogen-doped mesoporous carbon of extraordinary capacitance for electrochemical energy storage. *Science, 350*, 1508–1513.
122. Deng, X., Zhao, B., Zhu, L., & Shao, Z. (2015). Molten salt synthesis of nitrogen-doped carbon with hierarchical pore structures for use as high-performance electrodes in supercapacitors. *Carbon, 93*, 48–58.
123. Wang, Z., Yan, T., Fang, J., Shi, L., & Zhang, D. (2016). Nitrogen-doped porous carbon derived from a bimetallic metal–organic framework as highly efficient electrodes for flow-through deionization capacitors. *Journal of Materials Chemistry A, 4*, 10858–10868.
124. Liu, Y., et al. (2015). Nitrogen-doped electrospun reduced graphene oxide–carbon nanofiber composite for capacitive deionization. *Rsc Advances, 5*, 34117–34124.
125. Shi, J., et al. (2014). Nitrogen and sulfur co-doped mesoporous carbon materials as highly efficient electrocatalysts for oxygen reduction reaction. *Electrochimica Acta, 145*, 259–269.
126. Ling, Z., et al. (2015). Boric acid-mediated B, N-codoped chitosan-derived porous carbons with a high surface area and greatly improved supercapacitor performance. *Nanoscale, 7*, 5120–5125.
127. Zhang, J., Zhou, J., Wang, D., Hou, L., & Gao, F. (2016). Nitrogen and sulfur codoped porous carbon microsphere: A high performance electrode in supercapacitor. *Electrochimica Acta, 191*, 933–939.
128. He, Z., et al. (2018). N, P co-doped carbon microsphere as superior electrocatalyst for VO^{2+}/VO^{2+} redox reaction. *Electrochimica Acta, 259*, 122–130.

129. Ding, M., et al. (2018). Rod-like nitrogen-doped carbon hollow shells for enhanced capacitive deionization. *FlatChem, 7*, 10–17.
130. Li, Y., et al. (2016). N-doped hierarchical porous carbon derived from hypercrosslinked diblock copolymer for capacitive deionization. *Separation and Purification Technology, 165*, 190–198.
131. Liu, X., et al. (2019). Nitrogen-doped hierarchical porous carbon aerogel for high-performance capacitive deionization. *Separation and Purification Technology, 224*, 44–50.
132. Min, X., Hu, X., Li, X., Wang, H., & Yang, W. (2019). Synergistic effect of nitrogen, sulfur-codoping on porous carbon nanosheets as highly efficient electrodes for capacitive deionization. *Journal of Colloid and Interface Science, 550*, 147–158.
133. Zhao, S., et al. (2016). High capacity and high rate capability of nitrogen-doped porous hollow carbon spheres for capacitive deionization. *Applied Surface Science, 369*, 460–469.
134. Yasin, A. S., Jeong, J., Mohamed, I. M., Park, C. H., & Kim, C. S. (2017). Fabrication of N-doped & SnO_2-incorporated activated carbon to enhance desalination and bio-decontamination performance for capacitive deionization. *Journal of Alloys and Compounds, 729*, 764–775.
135. Li, Y., et al. (2018). Design of nitrogen-doped cluster-like porous carbons with hierarchical hollow nanoarchitecture and their enhanced performance in capacitive deionization. *Desalination, 430*, 45–55.
136. Xu, X., et al. (2019). Capacitive deionization using nitrogen-doped mesostructured carbons for highly efficient brackish water desalination. *Chemical Engineering Journal, 362*, 887–896.
137. Xu, D., Tong, Y., Yan, T., Shi, L., & Zhang, D. (2017). N, P-codoped meso-/microporous carbon derived from biomass materials via a dual-activation strategy as high-performance electrodes for deionization capacitors. *ACS Sustainable Chemistry & Engineering, 5*, 5810–5819.
138. Liu, J., Lu, M., Yang, J., Cheng, J., & Cai, W. (2015). Capacitive desalination of ZnO/activated carbon asymmetric capacitor and mechanism analysis. *Electrochimica Acta, 151*, 312–318.
139. Zheng, F., Yang, Y., & Chen, Q. (2014). High lithium anodic performance of highly nitrogen-doped porous carbon prepared from a metal-organic framework. *Nature Communications, 5*, 5261.
140. Liu, T., Li, X., Zhang, H., & Chen, J. (2018). Progress on the electrode materials towards vanadium flow batteries (VFBs) with improved power density. *Journal of Energy Chemistry, 27*, 1292–1303.
141. Oh, K., Won, S., & Ju, H. (2015). Numerical study of the effects of carbon felt electrode compression in all-vanadium redox flow batteries. *Electrochimica Acta, 181*, 13–23.
142. Chang, T.-C., Zhang, J.-P., & Fuh, Y.-K. (2014). Electrical, mechanical and morphological properties of compressed carbon felt electrodes in vanadium redox flow battery. *Journal of Power Sources, 245*, 66–75.
143. Park, S.-K., et al. (2014). The influence of compressed carbon felt electrodes on the performance of a vanadium redox flow battery. *Electrochimica Acta, 116*, 447–452.
144. Lado, J. J., Pérez-Roa, R. E., Wouters, J. J., Tejedor-Tejedor, M. I., & Anderson, M. A. (2014). Evaluation of operational parameters for a capacitive deionization reactor employing asymmetric electrodes. *Separation and Purification Technology, 133*, 236–245.
145. Gao, X., et al. (2016). Complementary surface charge for enhanced capacitive deionization. *Water research, 92*, 275–282.
146. 146Biesheuvel, P., Suss, M. & Hamelers, H. (2015). Theory of water desalination by porous electrodes with fixed chemical charge. *arXiv preprint arXiv:1506.03948*.
147. Zhao, R., Biesheuvel, P., Miedema, H., Bruning, H., & Van der Wal, A. (2009). Charge efficiency: A functional tool to probe the double-layer structure inside of porous electrodes and application in the modeling of capacitive deionization. *The Journal of Physical Chemistry Letters, 1*, 205–210.
148. Cohen, I., Avraham, E., Noked, M., Soffer, A., & Aurbach, D. (2011). Enhanced charge efficiency in capacitive deionization achieved by surface-treated electrodes and by means of a third electrode. *The Journal of Physical Chemistry C, 115*, 19856–19863.
149. Wu, T., et al. (2015). Asymmetric capacitive deionization utilizing nitric acid treated activated carbon fiber as the cathode. *Electrochimica Acta, 176*, 426–433.
150. Omosebi, A., Gao, X., Rentschler, J., Landon, J., & Liu, K. (2015). Continuous operation of membrane capacitive deionization cells assembled with dissimilar potential of zero charge electrode pairs. *Journal of Colloid and Interface Science, 446*, 345–351.
151. Wouters, J. J., Lado, J. J., Tejedor-Tejedor, M. I., Perez-Roa, R., & Anderson, M. A. (2013). Carbon fiber sheets coated with thin-films of SiO_2 and γ-Al_2O_3 as electrodes in capacitive deionization: Relationship between properties of the oxide films and electrode performance. *Electrochimica Acta, 112*, 763–773.
152. Gao, X., Omosebi, A., Landon, J., & Liu, K. (2014). Enhancement of charge efficiency for a capacitive deionization cell using carbon xerogel with modified potential of zero charge. *Electrochemistry Communications, 39*, 22–25.
153. Gao, X., Omosebi, A., Landon, J., & Liu, K. (2015). Enhanced salt removal in an inverted capacitive deionization cell using amine modified microporous carbon cathodes. *Environmental Science & Technology, 49*, 10920–10926.
154. Ma, D., Wang, Y., Han, X., Xu, S., & Wang, J. (2017). Electrode configuration optimization of capacitive deionization cells based on zero charge potential of the electrodes. *Separation and Purification Technology, 189*, 467–474.
155. Algharaibeh, Z., & Pickup, P. G. (2011). An asymmetric supercapacitor with anthraquinone and dihydroxybenzene modified carbon fabric electrodes. *Electrochemistry Communications, 13*, 147–149.
156. Gao, H., Xiao, F., Ching, C. B., & Duan, H. (2012). High-performance asymmetric supercapacitor based on graphene hydrogel and nanostructured MnO_2. *ACS Applied Materials & Interfaces, 4*, 2801–2810.
157. Yan, J., et al. (2012). Advanced asymmetric supercapacitors based on Ni $(OH)_2$/graphene and porous graphene electrodes with high energy density. *Advanced Functional Materials, 22*, 2632–2641.
158. Gao, X., et al. (2019). Capacitive deionization using symmetric carbon electrode pairs. *Environmental Science: Water Research & Technology, 5*, 660–671.
159. He, F., Biesheuvel, P., Bazant, M. Z., & Hatton, T. A. (2018). Theory of water treatment by capacitive deionization with redox active porous electrodes. *Water Research, 132*, 282–291.
160. Yu, F., Wang, L., Wang, Y., Shen, X., Cheng, Y., & Ma, J. (2019). Faradaic reactions in capacitive deionization for desalination and ion separation. *Journal of Materials Chemistry A*, *7*(27), 15999–16027.
161. Achilleos, D. S., & Hatton, T. A. (2016). Selective molecularly mediated pseudocapacitive separation of ionic species in solution. *ACS Applied Materials & Interfaces, 8*, 32743–32753.

Peter Adeniyi Alaba does research in Catalysis, Electrochemistry, Renewable Energy and Advanced Environmental engineering, Data Analytics, Artificial Intelligence (AI). He is a graduate of Chemical Engineering from the Federal University of Technology, Minna (2006), building up with an M.Eng.Sc. from University of Malaya, (2016). He is a PhD candidate of University of Malaya. Peter is an author and has worked in collaboration with several scientists from Australia, Malaysia, Mexico, Canada, United Kingdom, Nigeria, etc. He also renders professional services to academic journals such as American Chemical Society (ACS) journals, Chemical Papers, Separation and Purification Technology, Industrial and Engineering Chemistry, Applied Water Science, Journal of Cleaner Production and African Journal of Biotechnology. He is currently a grant peer-review international expert for Estonian Research Council and National Center of Science and Technology Evaluation, JSC, Almaty, Kazakhstan. He is a corporate member of COREN (Council for the Regulation of Engineering in Nigeria).

Shaukat Ali Mazari earned a PhD Degree in Chemical Engineering from the Department of Chemical Engineering, University of Malaya, Kuala Lumpur Malaysia in 2016. Currently he works as an Assistant Professor in the Department of Chemical Engineering and Director Postgraduate Studies at Dawood University of Engineering and Technology, Karachi, Pakistan. He works on process design, modeling and simulation for post-combustion CO_2 capture, CO_2 utilization, solvent development for CO_2 capture, CO_2 reduction into useful products, wastewater treatment, and biomass conversion into fuels and chemicals. He has also been working on research projects related to nanotechnology and nanomaterials, their applications, and environmental concerns.

Hamisu Umar Farouk holds B. Engr. Chemical Engineering (1999) and M. Sc. Chemical Engineering (2005) from Ahmadu University Zaria, Kaduna sate, Nigeria. He obtained his PhD in Chemical Engineering (2019) from University of Malaya, Kuala Lumpur. He is currently a Lecturer I, Department of Pure and Industrial Chemistry, Faculty of Physical Science, Bayero University Kano, Kano State, Nigeria (2008 – date). His skills include Lecturing, photocatalysis, surface analysis of materials, Natural gas pipeline transportation using Geographic Information System (GIS), Base knowledge of electricity Billing System, Laboratory scale catalytic cracking of cyclohexane, Computational Materials Physics with interest in Density functional theory (DFT) (in progress). He has membership of many Professional Bodies such as Council for Regulation of Engineering in Nigeria, Nigerian Society of Engineers, Nigerian Society of Chemical Engineers, Institute of Chattered Chemists. He accessed two grants leading to publication of many journal papers in high impact category.

Samuel Eshorame Sanni is a lecturer in the Department of Chemical Engineering of Covenant University. He is an astute researcher with outstanding contributions in Engineering Sciences. He has authored and co-authored over 64 publications indexed in reputable outlets (Scopus & Web of Science). His research competencies include: Process Engineering, Energy and Fuels, Chemical Reaction Engineering, Surface Electrochemistry and Materials Science.

Oluranti Agboola is a researcher and senior lecturer in the Department of Chemical Engineering, Covenant University, Ota, Nigeria. She obtained her first academic degree; Bachelor of Engineering, Chemical Engineering from the Department of Chemical Engineering, Federal University of Technology, Minna, Niger State. Nigeria. She obtained M. Tech & D. Tech. Chemical Engineering, from the Department of Chemical, Metallurgical and Materials Engineering; Tshwane University of Technology, South Africa. Her main research interests are in Modeling and Simulation, polymeric membrane and nanotechnology for desalination, polymer technology and corrosion science. She has over 358 Google Scholar citations, h-index of 8 and i-10 index of 8. She has authored over 96 publications with 63 indexed in Scopus with Scopus index of 5.

Ching Shya Lee is current a business development and commercialisation officer. She hold her first degree in Applied Chemistry from University of Malaya in 2003. Later, she gained her Master Degree from University of Putra Malaysia in 2008 with a scholarship sponsored by Malaysian Palm Oil Board (MPOB). Her master thesis was working on the research in Organic Synthesis and Oleochemicals studies. Then, she pursued my PhD degree in Chemical Engineering, majoring in Electrochemistry. Her research project is to study the electrochemical conversion of glycerol into various added-value compounds. She is a Dual PhD holder, graduated from University of Toulouse, France and University of Malaya, Malaysia. Her thesis was nominated by the Jury to participate

in the Prix Leopold Escande competition to compete for the top ten thesis in Toulouse. Her main research interests are in organic synthesis, electrochemistry, reaction engineering, separation processes and wastewater treatment.

Faisal Abnisa is a Doctor in Chemical Engineering from University of Malaya, Malaysia. He has been actively involved in the research of pyrolysis of biomass since 2008 and has published extensively. He also worked as a Postdoctoral Research Fellow in the Department of Chemical Engineering, University of Malaya. Currently, he is an associate professor in the Department of Chemical Engineering and Materials Engineering, Faculty of Engineering, King Abdulaziz University, Saudi Arabia. His research interests focus on the conversion of wastes to value-added chemicals, as well as thermal conversion of biomass and the use of pyrolysis liquid for fuel and chemical products.

Mohamed Kheireddine Aroua holds a Degree in Chemical Engineering from Tunisia and a Master in Material Sciences and Engineering from the University of Nancy 1, France. He obtained his Ph.D. in Analytical Chemistry in 1992 from the University of Nancy I, France. He joined the Department of Chemical Engineering, University of Malaya in 1993 as a lecturer and was promoted to Associate Professor in 2002, then to a Professor in 2007 and to a senior Professor in 2010. He was appointed as the Deputy Dean of the Institute of Graduate Studies from May 2009 until July 2016 and Head of the Department of Chemical Engineering at the Faculty of Engineering from 2016 to 2017. In addition, he has been the Head of the Center for Separation Science and Technology (CSST) from 2012 to 2017. Currently he is a Professor with Sunway University, Malaysia and Lancaster University in UK. On 2nd January 2018, he was appointed as Honorary Professor at University of Malaya.Recently he has established the Centre for Carbon Dioxide Capture and Utilization (CCDCU) at Sunway University.

Wan Mohd Ashri Wan Daud received his Bachelor degree in Chemical Engineering from Leeds University, UK in 1991. He earned a Master of Engineering in the field of combustion science and pollution control and PhD in reaction engineering from University of Sheffield , UK in 1993 and 1996 respectively. He joined University of Malaya under SLAB programme in 1993 and became a permanent staff in 1996. In 2003 he was promoted to Associate Professor and in 2018 he became a full professor. His research interests include activated carbon, hydrogen production, biodiesel production, hydrodeoxygenation of pyrolytic oil and electrocatalysis process. He has been awarded a number of research grants which include IRPA grant in 1997, UM High Impact research grant in 2011 and 'Sanjungan' grant in 2015 by Ministry of Higher Education. He was appointed as the head of the department of Chemical Engineering from 2011 to 2013 and Dean for Advanced Science and Technology Cluster from 2013 to 2014. Besides was the Head of the Center for Separation Science and Technology (CSST) from 2009 to 2012.